# Persistent collapse of biomass in Amazonian forest edges following deforestation leads to unaccounted carbon losses

**Article** *in* Science Advances · September 2020

DOI: 10.1126/sciadv.aaz8360

CITATIONS
80

READS
901

**13 authors**, including:

Celso H. L. Silva-Junior
University of California, Los Angeles
**108** PUBLICATIONS **1,576** CITATIONS
SEE PROFILE

Luiz E. O. C. Aragão
National Institute for Space Research, Brazil
**446** PUBLICATIONS **26,149** CITATIONS
SEE PROFILE

Liana O. Anderson
Centro Nacional de Monitoramento e Alertas de Desastres Naturais
**282** PUBLICATIONS **9,743** CITATIONS
SEE PROFILE

Marisa Gesteira Fonseca
**33** PUBLICATIONS **1,323** CITATIONS
SEE PROFILE

APPLIED ECOLOGY

# Persistent collapse of biomass in Amazonian forest edges following deforestation leads to unaccounted carbon losses

Celso H. L. Silva Junior[1,2]*, Luiz E. O. C. Aragão[1,2,3], Liana O. Anderson[1,4], Marisa G. Fonseca[1,2,5], Yosio E. Shimabukuro[1,2], Christelle Vancutsem[6], Frédéric Achard[6], René Beuchle[6], Izaya Numata[7], Carlos A. Silva[8], Eduardo E. Maeda[9], Marcos Longo[10], Sassan S. Saatchi[10,11]



**Deforestation is the primary driver of carbon losses in tropical forests, but it does not operate alone. Forest fragmentation, a resulting feature of the deforestation process, promotes indirect carbon losses induced by edge effect. This process is not implicitly considered by policies for reducing carbon emissions in the tropics. Here, we used a remote sensing approach to estimate carbon losses driven by edge effect in Amazonia over the 2001 to 2015 period. We found that carbon losses associated with edge effect (947 Tg C) corresponded to one-third of losses from deforestation (2592 Tg C). Despite a notable negative trend of 7 Tg C year$^{-1}$ in carbon losses from deforestation, the carbon losses from edge effect remained unchanged, with an average of 63 ± 8 Tg C year$^{-1}$. Carbon losses caused by edge effect is thus an additional unquantified flux that can counteract carbon emissions avoided by reducing deforestation, compromising the Paris Agreement's bold targets.**

## INTRODUCTION

Tropical forests play a crucial role in the global carbon cycle, with carbon stocks varying between 193 and 229 Pg (*1*, *2*), representing about 54% of the global aboveground carbon (AGC) stock (*3*). The area of these forests, however, declined by 10%, from 19.65 million km$^2$ in 1990 to 17.70 million km$^2$ in 2015, because of land-use and land-cover changes (*4*). The magnitude of these forest changes affects essential ecosystem services, including carbon storage, biodiversity, climate regulation, nutrient cycling, and water supply (*5*, *6*).

In Amazonia, the world's largest continuous tropical forest, deforestation has continuously converted old-growth forests into agricultural and livestock areas, fragmenting the landscape extensively. Forest fragmentation is associated with the increased number of forest patches and augmentation of the extent of forest edges perimeter and area (*7*, *8*). These changes in forest cover configuration cause direct carbon losses from edge effect and agricultural fire incursion into adjacent stand forests (*8*–*15*). The exposure of the Earth's forests to edge effect is widespread (*16*–*18*). Globally, about 70% of forests were within 1 km of forest edges in 2000 (*19*). However, only 5.2% of the forests in the Brazilian Amazon were in this same edge zone in 2014 (*7*).

Pioneering investigations from the BDFFP (Biological Dynamics of Forest Fragments Project), in the Brazilian Central Amazon, found significant carbon losses at forest edges (depth of 100 m) induced by microclimatic changes, leading to increased tree mortality rates.(*9*–*11*). However, the magnitude of carbon losses at these forest edges is still poorly quantified at large scales due to the scarcity of quantitative datasets for tropical forests. Efforts to accurately incorporate this source to regional and global carbon budgets are urgently needed for improving the estimations of the contribution of land-use and land-cover changes to the atmospheric carbon burden. This quantification is critical for the effectiveness of sustainable development policies and must be explicitly included either in national greenhouse gas inventories of tropical countries or in REDD+ (reducing emissions from deforestation and degradation) reports (*20*). Initial attempts were already made to quantify the carbon losses caused by edge effect in Amazonia (*21*–*27*); nonetheless, these studies were constrained by the availability of synoptic data, the accuracy of models, the spatial resolution of the remote sensing data used, or the study area extent.

Representing the environmental variability of edge effect and associated carbon stocks across Amazonia is a challenge due to its large area. In this context, remote sensing technologies play an essential role in quantifying both the extent of fragmentation-induced forest edges and the negative impact of edge effect on forest carbon stocks. The recent availability of 30-m spatial resolution forest change datasets (*28*) based on optical images from the Landsat series of Earth Observation satellites provides a unique opportunity to quantify forest edge extent and age in detail at pan-Amazonia scale. This information integrated with airborne LiDAR (light detection and ranging) technology collected over Amazonian forests offers a powerful combination for estimating forest carbon stocks in these areas, based on accurate models of forest structure (Fig. 1) (*29*, *30*).

Therefore, in this study, we aim to provide a unique spatially and temporally explicit quantification of carbon losses from forest edges and estimate the additional contribution to gross deforestation-induced carbon losses. Specifically, we (i) analyzed 16 years (2000–2015) of readily available 30-m spatial resolution Landsat-based forest cover and change datasets (*28*) to quantify the dynamics and age distribution

[1]Tropical Ecosystems and Environmental Sciences Laboratory, São José dos Campos, SP, Brazil. [2]Remote Sensing Division, National Institute for Space Research, São José dos Campos, SP, Brazil. [3]Geography, College of Life and Environmental Sciences, University of Exeter, Exeter, UK. [4]National Center for Monitoring and Early Warning of Natural Disasters, São José dos Campos, SP, Brazil. [5]Veraterra–Mapping and Environmental Consultancy, Praça Pedro Gomes, s/n, Serra Grande, Uruçuca, BA 45680-000 Brazil. [6]European Commission, Joint Research Centre (JRC), 21027 Ispra, Italy. [7]Geospatial Sciences Center of Excellence, South Dakota State University, Brookings, SD, USA. [8]School of Forest Resources and Conservation, University of Florida, Gainesville, FL 32611, USA. [9]Department of Geosciences and Geography, Faculty of Science, University of Helsinki, Helsinki, Finland. [10]Jet Propulsion Laboratory, California Institute of Technology, Pasadena, CA 91109, USA. [11]Institute of the Environment and Sustainability, University of California, Los Angeles, CA 90024, USA.
*Corresponding author. Email: celsohlsj@gmail.com

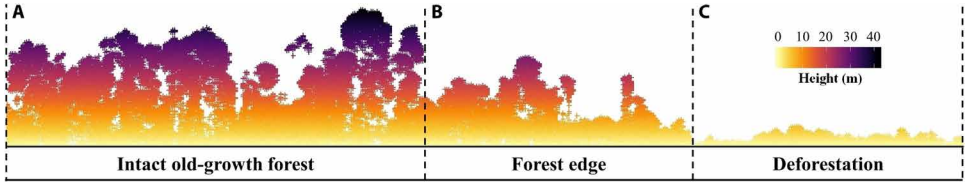


**Fig. 1. LiDAR point cloud profile.** Point cloud data collected in 2014 in the northeast of the Pará state, Brazil with 420 m of length. The points represent the vegetation height, which was normalized by the terrain altimetry. (**A**) Structure of a nondegraded old-growth forest, where the trees height reaches up to 40 m. (**B**) Forest edge (width of 120 m), where the height of the vegetation reaches up to 25 m. (**C**) Deforested area with vegetation regrowth (height up to 5 m).

of forest edges in Amazonia, (ii) processed an airborne LiDAR dataset collected across several locations in the studied area to build an empirical carbon loss model as a function of forest edge age, and last, (iii) modeled the edge-induced carbon loss across the entire Amazonia by applying the LiDAR-based carbon loss model across all pixels of the forest edge age maps. Our model is grounded on the observation (*31*) and concept (*32*) that tropical forest edges formed by deforestation continuously reduce their carbon stocks with age. Thus, we hypothesize that direct carbon losses by deforestation are followed by incremental indirect carbon losses induced by the aging of forest edges in Amazonia.

## RESULTS

### Forest edge dynamics and age distribution

The dynamics of forest edges creation and erosion (defined here as the complete removal of canopy cover of the forest edge) is explained directly by the pattern and pace of deforestation. In Fig. 2, we present our findings regarding Amazonian forest edges dynamics (Fig. 2, A and B) and their age distribution (Fig. 2, C and D). We estimate that 5% of the standing forest cover in 2000 was deforested between 2001 and 2015, or a gross forest loss of 273,195 $km^2$, at an average of 18,213 ± 4303 $km^2$ $year^{-1}$ (Fig. 2A). We observed a deforestation peak of 26,376 $km^2$ in 2004 and a minimum value in 2013 (12,578 $km^2$). However, the Mann-Kendall test (MK) showed that annual deforestation overall decreased significantly at a rate of 683 $km^2$ $year^{-1}$ (MK = −0.49 and $P < 0.05$) along the 15-year period.

During the interval studied, Brazil was the country with the highest deforestation rate (14,835 ± 4706 $km^2$ $year^{-1}$), contributing with an average of 62 ± 10% $year^{-1}$ of overall deforestation in Amazonia (fig. S1). Brazil is also the leader in relative contribution rate (percentage of annual deforestation in relation to Amazonia area of each country), with an average of 0.355 ± 0.109% $year^{-1}$ (table S1). In contrast, French Guiana had the lowest deforestation rate (33 ± 18 $km^2$ $year^{-1}$), contributing with an average of 0.20 ± 0.10% $year^{-1}$ of overall Amazonian deforestation, with a relative contribution rate average of 0.040 ± 0.021% $year^{-1}$ (table S1). However, across all Amazonian countries, only Brazil had a significant negative temporal trend in deforestation, at a rate of 773 $km^2$ $year^{-1}$ (MK = −0.55 and $P < 0.05$), while Peru had the highest significant temporal trend of increase, at a rate of 68 $km^2$ $year^{-1}$ (MK = 0.67 and $P < 0.05$). Details about annual deforestation rates and temporal trends for all countries in the Amazonia can be found in fig. S1 and tables S1 and S2.

In 2015, we estimated that forests edges, considering a depth of 120 m (*10*, *33*), covered an area of 176,555 $km^2$ across the whole Amazonia (Fig. 2A). This represents about 65% of the total deforested area between 2001 and 2015 or 3% of the total forest area in 2015 over the region. On average, 11,770 ± 3546 $km^2$ $year^{-1}$ of new forest edges were created in Amazonia, with a maximum area of 17,815 $km^2$ in 2012 and a minimum of 6481 $km^2$ in 2011 (Fig. 2A). Brazil and Peru had the highest annual edge creation average, contributing with 7600 ± 3427 $km^2$ $year^{-1}$ and 1510 ± 300 $km^2$ $year^{-1}$, respectively. In addition, we quantified that on average, 7 ± 1, 24 ± 4, and 42 ± 3% of the forest edges were eroded by forest-clearing process after 1, 5, and 10 to 14 years of their creation, respectively (Fig. 2B).

Similar to the patterns found for deforestation rates in the Amazonia, the creation of forest edges decreased significantly at a rate of 707 $km^2$ $year^{-1}$ (MK = 0.74 and $P < 0.05$) between 2001 and 2015 (Fig. 2A). Across all Amazonian countries (table S1), Brazil and Colombia had a significant decreased trend in edge formation ($P < 0.05$), with rates of 683 and 49 $km^2$ $year^{-1}$, respectively. Conversely, Guyana and Suriname had a significant increased trend ($P < 0.05$), with rates of 5 and 11 $km^2$ $year^{-1}$, respectively. Details about temporal trends of forest edge dynamics for Amazonian countries are shown in fig. S2 and table S3.

In 2015, we observed that the oldest edges (between 10 and 15 years old) were distributed mainly over the Brazilian Arc of Deforestation (*34*), an old Amazonian deforestation frontier located in the southeast flank of Amazonia (Fig. 2C). We also observed old forest edges in the southern portion of Bolivia and in the north of Amazonia, including three countries: Colombia, Venezuela, and Guyana. On the other hand, the youngest forest edges (between 1 and 3 years old) dominated not only the new active deforestation frontiers in southern Bolivia, western Peru, and northern Colombia but also areas in the central Brazilian Amazon.

On average, forest edges in Amazonia were 7 ± 3 years old in 2015. The edge age distribution was close to uniform: 23% of the forest edges ages were between 1 and 3 years, 21% between 4 and 6 years, 19% between 7 and 9 years, 20% between 10 and 12 years, and 16% between 13 and 15 years. Considering all Amazonian countries, the age of forest edges spanned from an average of 6 ± 3 years in Suriname to 8 ± 3 years in Colombia (Fig. 2D and Table 1). The Kruskal-Wallis test (KW) showed a significant difference (KW = 1179 and $P < 0.05$) in the age of forest edges among the Amazonian countries (Fig. 2D). For instance, we found that forest edge age was significantly ($P < 0.05$) lower in Suriname (group e) and higher in Colombia (group a). However, the age of forest edges in the pair Brazil and Venezuela (group b) and in the group Ecuador, Guyana, and Peru (group d) was statistically indistinguishable from each other. Last, the age of forest edges in French Guiana (cd group) was not distinguishable from countries belonging to groups c and d, simultaneously.

### Spatial-temporal variation in AGC losses

By combining the age information from the mapped forest edges with the airborne LiDAR data, we established a relationship depicting

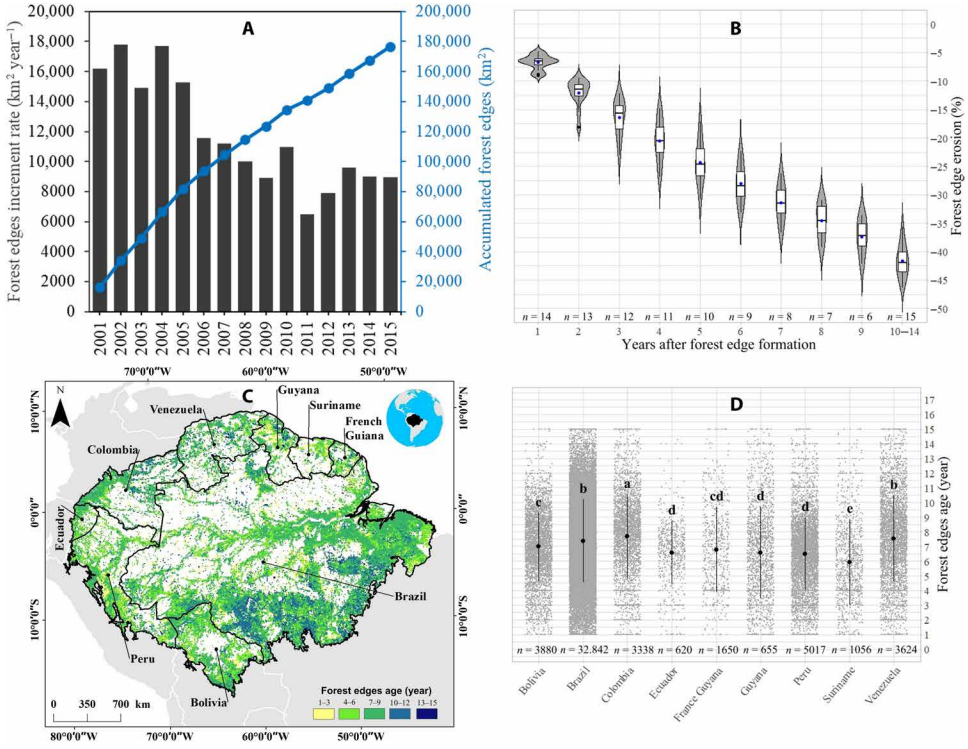


**Fig. 2. Forest edges creation, erosion, and age composition in Amazonia.** (**A**) Temporal forest edges variation in Amazonia, where the black bars are the annual forest edges increment rate and the blue line is the total gross forest area increment from 2001. (**B**) Boxplots of forest edges erosion rates (as a negative percentage) for Amazonia, where the bold horizontal lines are the medians, the blue dots are the averages, the shaded area is the frequency distribution function, and *n* is the number of observations. (**C**) Spatial distribution of forest edges age in 2015 in Amazonia; ages were aggregated by the average in a 10 km by 10 km grid cell to improve visualization. (**D**) Dot plots of forest edge age [each dot corresponds to a single grid cell in (C)] in Amazonian countries in 2015, where the vertical bars are the SDs, the black dots are the averages, the gray dots are the data observations, and *n* is the number of observations. The letters in bold represent the groups defined by the post hoc test.

**Table 1. Average and median of the forest edges ages for the Amazonian countries.**

| Country | Forest edges ages (years) | |
|---|---|---|
| | Average ± SD | Median |
| Bolivia | 7.00 ± 2.35 | 7.01 |
| Brazil | 7.38 ± 2.84 | 7.54 |
| Colombia | 7.67 ± 2.88 | 7.96 |
| Ecuador | 6.58 ± 2.17 | 6.84 |
| France Guyana | 6.57 ± 3.11 | 6.41 |
| Guyana | 6.78 ± 2.91 | 6.57 |
| Peru | 6.48 ± 2.50 | 6.56 |
| Suriname | 5.94 ± 2.93 | 5.49 |
| Venezuela | 7.53 ± 2.94 | 7.59 |

the loss of aboveground forest carbon as a function of the age of forest edges (see Materials and Methods) to investigate the spatial and temporal changes of carbon stocks associated with edge effect across Amazonia. As shown in Fig. 3 (A and B) between 2001 and 2015, carbon losses related to edge effect ranged from 0.001 up to 0.252 Tg C per grid cell (100 $km^2$), while losses from deforestation ranged from 0.001 up to 0.799 Tg C per grid cell. More than 60% of the grid cells had values of carbon loss varying between 0.001 and 0.022 Tg C, both for edge effect and deforestation (Fig. 3, C and D). Spatially, absolute carbon loss values associated with edge effect and deforestation presented similar patterns across Amazonia (Fig. 3, A and B), with substantial accumulated losses over the Brazilian Arc of Deforestation (*34*) and the southwest Amazonian flank. The lower accumulated losses were spatially distributed over the central and the northern part of Amazonia.

Figure 3E shows the relative contribution of edge effect and deforestation for the total carbon loss between 2001 and 2015 as a percentage of each grid cell. We found that relative contribution of edge effect and deforestation for the carbon loss of grid cells were heterogeneous across Amazonia during the studied period. While carbon losses from edge effect dominated mainly the central Amazonia region, carbon loss associated with deforestation were more evident along the Brazilian Arc of Deforestation (*34*) and areas in Peru, Bolivia, and southern French Guiana.

Between 2001 and 2015, we estimated a total gross carbon loss from edge effect of 947 Tg C (0.95 Pg C), with an average of 63 ± 8 Tg C $year^{-1}$ between 2001 and 2015 in Amazonia. We did not identify any temporal trend in the time series (Sen's slope = −0.22 Tg C $year^{-1}$, MK = −0.01, and $P > 0.05$). We observed a carbon loss peak of 78 Tg C in 2005, while we recorded a minimum loss of 41 Tg C related to edge effect in 2001 (Fig. 4A). In contrast, the total gross carbon loss from deforestation was 2592 Tg C (2.59 Pg C), with an average of 173 ± 46 Tg C $year^{-1}$, and a significant negative temporal trend of

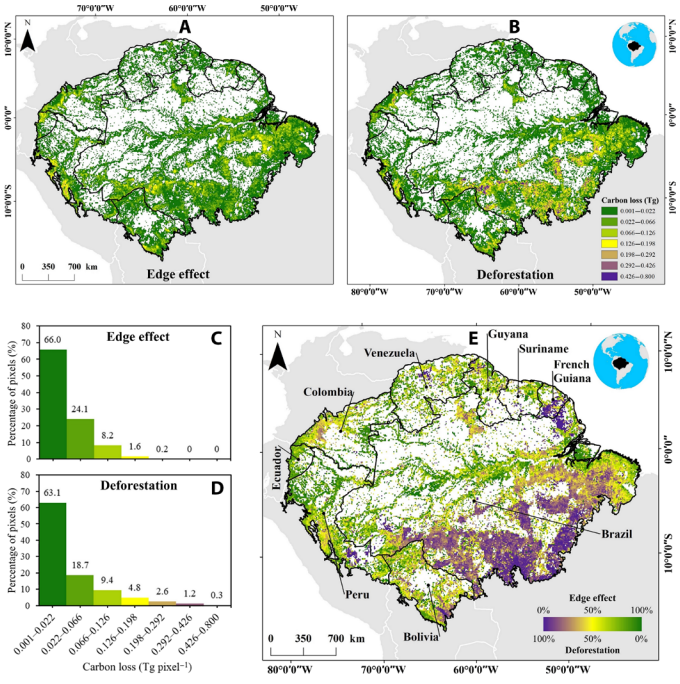


**Fig. 3. Spatial variability of carbon losses in Amazonia.** Spatial variability of carbon losses between 2001 and 2015 from (**A**) edge effect and (**B**) deforestation. Histograms of frequency distribution of carbon losses related to (**C**) the edge effect presented in (A) and (D) the deforestation presented in (B). (**E**) Percent contribution of edge effect and deforestation to the total carbon loss of each pixel in Amazonia. Carbon losses were aggregated by the sum in a 10 km by 10 km grid cell to improve visualization in (A) and (B).

6.90 Tg C year$^{-1}$ (MK = −0.51 and $P < 0.05$) between 2001 and 2015. Unlike the observed pattern of carbon loss from forest edges, the peak of deforestation-related carbon loss occurred in 2004 (261 Tg C), and the minimum was recorded in 2013 (114 Tg C) (Fig. 4B). Across all Amazonian countries, Brazil had the most substantial contribution for the Amazonia-wide carbon loss from both forest edges and deforestation, representing an average of 67 ± 6% year$^{-1}$ and 79 ± 7% year$^{-1}$, respectively (Fig. 4, A and B). At the same time, Suriname's forest edges and deforestation had the lowest contribution, with an average of 1.03 ± 0.57% year$^{-1}$ and 0.48 ± 0.35% year$^{-1}$, respectively (Fig. 4, A and B).

Overall, our findings show that the deforestation process leads to a collateral carbon loss of 37% related to the dynamics of forest edges in the Amazonia. Most notably, unlike the carbon loss from deforestation, which declined significantly during the analyzed period, the additional carbon loss associated with the edge effect remained unchanged over time. Note that the difference between carbon losses from deforestation and edge effect decreased over time. In 2001, deforestation promoted a loss of 122 Tg C greater than that observed for the edges; however, in 2015, this difference decreased to 66 Tg C (fig. S3A). During the studied period, hence, the carbon loss from forest edges that contributed to 25% of the loss from deforestation in 2001 increased to 48% in 2015 (fig. S3B). In 2013, carbon loss induced by edge effect was more than half (54%) of the direct deforestation loss (fig. S3B).

The analysis of temporal trend and average of carbon losses associated with edge effect and deforestation across all Amazonian countries (Table 2) showed that Ecuador, Guyana, Peru, and Suriname had a significant ($P < 0.05$) positive trend in carbon losses, both by edge effect and deforestation, varying between 0.01 and 0.41 Tg C year$^{-1}$ for edge effect and between 0.01 and 0.65 Tg C year$^{-1}$ for deforestation. Only Brazil had a significant ($P < 0.05$) negative temporal trend of deforestation-associated carbon loss, although loss from edges remained unchanged ($P > 0.05$) over time. In contrast, Venezuela had a significant ($P < 0.05$) positive trend in carbon loss from deforestation, but losses from edge effect remained unchanged ($P > 0.05$) over time.

## DISCUSSION

### Trends in deforestation across Amazonian countries

From our approach, we observed a significant decline in forest clearing processes between 2001 and 2015 in Amazonia. This decline followed the reduction in the deforestation rates observed in Brazil. The reduction in deforestation rates observed here for the Brazilian portion of Amazonia corroborates the progressive decline reported by the official deforestation system operating in Brazil (fig. S1) (*35*). This reduction was a result of the strengthening of policies for prevention and control of deforestation in the region called Brazilian Legal Amazon, consolidated since the creation of the PPCDAm (Plano de Ação para Prevenção e Controle do Desmatamento na Amazônia Legal; Action Plan for Prevention and Control of Deforestation in the Legal Amazon) in 2004 (*36*). During the first three phases of the PPCDAm (2004–2015), policies were created and actions implemented, including the creation and consolidation of near–real time systems for monitoring deforestation based on remote sensing, the intensification of law enforcement, the restriction of credit for illegal loggers, the creation and consolidation of conservation units and indigenous lands, and advances in land policy, such as the Rural Environmental Registry (Cadastro Ambiental Rural) (*37*). However, from 2013 to 2019, an upward trend was observed in the official deforestation rates (*35*), marked by an impressive rate of 10,129 km$^2$ in 2019, an increase of 34% compared to 2018 (7536 km$^2$), the highest rate since 2008 (12,911 km$^2$). This upward trend was induced by environmental setbacks such as controversial changes in the Brazilian Forest Code in 2012 (*38*), the recent weakening of deforestation enforcement, the dismantling of climate change policies (including the interruption of the PPCDAm from 2019), and the possibility of regularization of public lands illegally grabbed (Bill n° 2633/2020, former Provisional Measure n° 910/2019) (*39*, *40*).

Although the PPCDAm was a key step for the reduction of the deforestation in the Brazilian Amazon, other external factors such as the soy and beef moratoria (*41*) also played a critical role. Companies associated with the agribusiness agreed upon an embargo on soy and beef produced in illegal deforested areas. All these policies and actions inhibited illegal deforestation activities in the Brazilian Amazon, resulting in the significant decline of deforestation rates in Brazil after 2004. This pattern drove the overall trend of deforestation reduction across Amazonia.

Countries such as Ecuador, Guyana, Peru, and Suriname had, however, a significant increase in deforestation rates between 2001 and 2015. In Ecuador, the deforested areas were associated with increased commodity prices between 2005 and 2014, intensifying mineral and hydrocarbon extraction, agriculture production, logging, and palm cultivation (*42*, *43*). In Guyana (*43*, *44*), Suriname (*43*, *45*), and Peru (*43*, *46*), on the other hand, the increase in

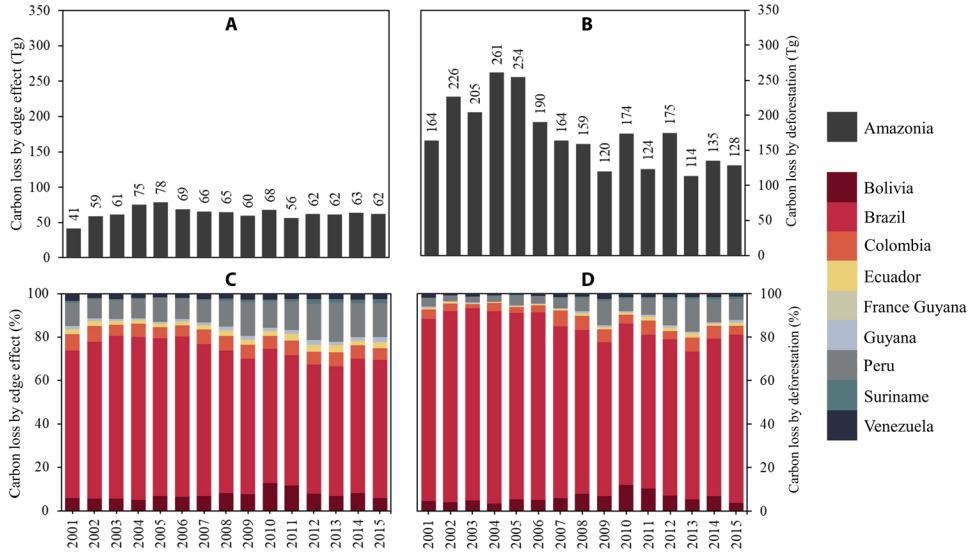


**Fig. 4. Temporal variability of carbon losses in Amazonia.** (**A**) Temporal carbon loss variability by fragmentation. (**B**) Temporal carbon loss variability by deforestation. The bottom panels show the contribution as a percentage of each country to the annual carbon loss by edge effect (**C**) and deforestation (**D**).

**Table 2. Temporal trend and average carbon losses induced by edge effect and deforestation for all Amazonian countries.** Where S is the Man-Kendell statistics. The S statistic with an asterisk (*) means a significant temporal trend at 95% of significance level ($P \leq 0.05$).

| Country | Edge effect | | | Deforestation | | |
|---|---|---|---|---|---|---|
| | S | Sen's slope (Tg C year$^{-1}$) | Average ± SD (Tg C year$^{-1}$) | S | Sen's slope (Tg C year$^{-1}$) | Average ± SD (Tg C year$^{-1}$) |
| Bolivia | 0.37 | 0.14 | 5 ± 1.41 | −0.03 | −0.02 | 10 ± 3.60 |
| Brazil | −0.31 | −0.58 | 42 ± 7.67 | −0.61* | −8.41 | 139 ± 47.68 |
| Colombia | −0.11 | −0.03 | 4 ± 0.47 | −0.15 | −0.02 | 8 ± 1.97 |
| Ecuador | 0.71* | 0.06 | 1 ± 0.34 | 0.51* | 0.08 | 1 ± 0.53 |
| France Guiana | 0.35 | 0.01 | 0 ± 0.06 | 0.15 | 0.01 | 0 ± 0.20 |
| Guyana | 0.71* | 0.04 | 1 ± 0.23 | 0.41* | 0.04 | 1 ± 0.28 |
| Peru | 0.73* | 0.41 | 8 ± 1.97 | 0.63* | 0.65 | 11 ± 4.25 |
| Suriname | 0.83* | 0.07 | 1 ± 0.36 | 0.75* | 0.07 | 1 ± 0.49 |
| Venezuela | 0.45* | 0.02 | 1 ± 0.17 | 0.09 | 0.01 | 2 ± 0.52 |

deforestation rates was mainly induced by activities related to illegal gold mining at different scales. Last, countries such as Bolivia, Colombia, French Guiana, and Venezuela had constant deforestation rates (no significant trends) between 2001 and 2015. These deforested areas were the result of agricultural, livestock, and mining activities (*43*, *44*, *47*, *48*), which potentiate the collateral impacts of edge effect on forest degradation and biodiversity loss (*49*).

## The collapse of AGC stocks in forest edges

Consistent with the decline in deforestation, we identified a significant decrease in the annual forest edge formation in Amazonia. The dynamics of forest edge formation result from the spatial and temporal patterns of deforestation, which defines the spatial arrangements and the geometries of the forest fragments (*50*, *51*). Landscapes arising from the deforestation process associated with the establishment of rural settlements (fish bone pattern) have up to five times more forest edge areas per deforested land than landscapes dominated by large (regular shape) farms (*51*). The average rate of erosion of 11.47% within 3 years after forest edges creation and its subsequent increase to 42.80% after 12 years, found in our study, are lower than those found in previous studies at the local scale in Amazonia (*22*, *50*). The lower rates found here are likely to be a result of two nonexclusive processes, including a significant decrease in deforestation rates and the creation of more regular shape deforested polygons.

The drivers and historical trends of deforestation and forest edge creation are country specific (*50*). Bolivia, Colombia, Venezuela, Peru, and Suriname presented a large proportion of forest edges areas with 1 to 6 years old, which is explained by the intensification of deforestation in these countries in recent years (*52*). The other Amazonian countries, as Brazil, have older forest edges areas, due to an older and more consolidate deforestation frontier, which stabilized by the end of the study period (*52*).

Our findings indicated that aboveground forest carbon progressively decreased in Amazonian forest edges as a function of their

ages (fig. S13). This pattern is corroborated by similar results found in Sabah, Malaysian Borneo (*31*). The losses observed in our study are greater in the first 5 years after the edge creation, which are consistent with field observations in controlled experiments in the Brazilian Central Amazon (fig. S4A) (*10*, *27*). Following forest edge formation, mortality rates increase significantly (fig. S5C), in particular among larger trees, which store most of the forest's carbon (*53*, *54*). In addition, microclimatic changes tend to increase wind turbulence and fire promoting an exacerbation of disturbance rates in the forest edges (*55*–*59*). Together, these effects cause a steep initial reduction in carbon stocks following the edge formation. Subsequently, with the aging of the edges, turnover rates (*60*), number of woody lianas (*10*), and pioneer species increase, as a result of the successional process (*33*). Following this process, the plant community established in the forest edge tends to be better adapted to the new microclimatic conditions, sealing the edges (fig. S5D) and reducing the susceptibility to further microclimatic changes (*56*, *61*–*63*). Although growth of new trees increases over time, turnover rates also increase (*64*), as a consequence of increasing mortality, so our age-carbon loss function (fig. S13) capture the tendency of forest edges to reach an alternative postfragmentation equilibrium state. This alternative state, which stabilizes between 6 and 15 years after the edge creation, is characterized by forests with lower aboveground biomass (AGB) than adjacent core areas. Field observations in controlled experiments in the Central Brazilian Amazon demonstrated a significant reduction in canopy height, basal area, and AGB of up to 10 years after edge formation (*27*). The relationship between distance to edge and AGB was, however, no longer significant after 22 years of edge formation (*27*). Differently from Almeida *et al.* (*27*), in our analyses, the AGB values are likely to remain below prefragmentation levels after 15 years, because most of the Amazonian forest edges are constantly exposed to the incidence of fire, which in the Brazilian Amazon can lead to a reduction in forest AGB of 24.8 ± 6.9% after 31 years (fig. S6) (*64*). We expect the recovery of Amazonian forest edges in few areas where secondary forests are growing adjacent to these edges; however, these areas are likely to be minor as secondary forests in the Brazilian Amazon are limited to 34% (in 2018) of the total deforested area (1988–2018 period) (*35*, *65*).

The estimated AGC losses in our study are considerably higher (24.93 ± 4.53% of difference) than those found by Laurance *et al.* (*10*) in the local scale BDFFP long-term experiment (fig. S4B). These differences are expected as our Amazonia-wide analysis captures variations in factors influencing the stability of AGC in forest edges not contemplated by controlled local-scale experiments such as: (i) multiple configurations of size, shape and types of land use, and land cover surrounding the forest edges (*66*) and mainly, (ii) the impact of fires on forest edges (*54*, *64*). In Amazonia, fire typically occurs in forest edges (*8*, *13*, *15*, *67*–*69*) by escaping from deforested areas, pastures, and agricultural fields and leaking into surrounding forests (*70*, *71*). Moreover, fire in forest edges often damages the remaining trees, increasing their vulnerability to strong wind events, enhancing tree mortality rates (*72*). Last, during the 21st century, Amazonia has been exposed to an increased frequency of extreme droughts (*73*, *74*), which may induce the reduction in forest carbon stocks, either by the direct effect of drought on tree mortality (*75*) or by the collateral effect of increased fire incidence at the forest edges during these extreme events (*76*–*78*).

### Implications for carbon emissions reduction policies

Here, we showed at Amazonian scale that forest carbon loss induced by edge effect was one-third of the carbon loss caused by deforestation during the 2001 to 2015 period. Furthermore, our trend analysis showed that although deforestation-related carbon loss decreased significantly between 2001 and 2015, edge effect–related carbon loss remained unchanged. Knowing that part of the carbon losses in the forest edges is emitted to the atmosphere following the decomposition process, our findings show that deforestation-induced edge effect can indirectly increase emissions from deforestation alone by 37%, with implications for policies aiming to reduce in carbon emissions by avoiding deforestation.

To show the impact of neglecting carbon losses from edge effect on the calculation of gross deforestation emissions (fig. S7), we compared (Wilcoxon's test) carbon losses from each process before (between 2001 and 2004) and after (between 2005 and 2015) the implementation of the PPCDAm (*36*). The PPCDAm was the central policy responsible for the decline in deforestation rates in the Brazilian Amazon (*35*, *36*). We found that annual carbon loss associated with deforestation alone decreases significantly (41%; $W = 40$ and $P = 0.02$) from 187 ± 21 Tg year$^{-1}$ in the pre-PPCDAm period to 111 ± 39 Tg year$^{-1}$ in the post-PPCDAm period. The annual carbon loss associated with edge effect, conversely, in the pre-PPCDAm phase (43 ± 6 Tg year$^{-1}$) was not statistically different ($W = 25$ and $P = 0.75$) from the value calculated for the post-PPCDAm period (40 ± 7 Tg year$^{-1}$).

Our analysis points to two critical issues: first, because the carbon loss induced by edge effect is persistent over time, even with deforestation slowing down, extra emissions from the newly formed edges reduce the effectiveness of actions for reducing carbon emissions by avoiding deforestation, such as the REDD+ policy. The inclusion of the edge effect process into systems for monitoring, reporting, and verifying emissions is, hence, crucial. Second, we show that reducing deforestation carbon loss does not change edge-induced carbon loss, indicating the need of new mechanisms to avoid or to compensate the potential carbon emissions associated with edge effect. These could be related to landscape planning, which is necessary to be implemented not only in Amazonian countries but also in other tropical countries such as Africa and Asia. Besides, the recent deforestation upward trend in the Brazilian Amazon has a negative implication, the increase in carbon losses from deforestation, directly, and edge effect induced by the creation of new forest edges.

Decreasing uncertainties in emissions estimates from land-use and land-cover change can support the establishment of more effective national actions, helping Amazonian countries to accomplish with emission reductions targets proposed at international climate agreements, such as the Paris Agreement. The Paris Agreement aims to establish volunteer emission reduction actions and targets by the signatory countries to be reached by 2025, to strengthen the global response to the threat of climate change (*79*). For combating the effects of climate change, it is critical to maintain the global average temperature rise below 2°C from preindustrial levels and efforts to limit the temperature increase to 1.5°C (*80*). To achieve this goal, there is a pressing need for a 45 and 100% reduction in greenhouse gas emissions by 2030 and 2055, respectively (*81*). Our results indicate that there is a significant missing source to be considered in the Amazonian carbon budget. Including carbon losses related to edge effect in regional and global carbon budgets is, hence, crucial for

accurately estimate the land-use and land-cover change contribution to the atmospheric carbon burden. In conclusion, carbon losses associated with the edge effect in Amazonia are an additional unquantified carbon flux that can counteract carbon emissions avoided by reducing deforestation, compromising the Paris Agreement's bold targets.

## MATERIALS AND METHODS

Our materials and methods are included in the following five steps: (i) forest cover mapping, (ii) identification of forest edges and quantification of age structure, (iii) carbon stock mapping from LiDAR data, (iv) carbon stock loss model by edge effect and deforestation, (v) statistical analysis, and (vi) sources of uncertainty. Detailed information about each of these steps is provided in the Supplementary Materials.

## SUPPLEMENTARY MATERIALS

Supplementary material for this article is available at http://advances.sciencemag.org/cgi/content/full/6/40/eaaz8360/DC1

## REFERENCES AND NOTES


1. A. Baccini, S. J. Goetz, W. S. Walker, N. T. Laporte, M. Sun, D. Sulla-Menashe, J. Hackler, P. S. A. Beck, R. Dubayah, M. A. Friedl, S. Samanta, R. A. Houghton, Estimated carbon dioxide emissions from tropical deforestation improved by carbon-density maps. *Nat. Clim. Chang.* **2**, 182–185 (2012).
2. S. S. Saatchi, N. L. Harris, S. Brown, M. Lefsky, E. T. A. Mitchard, W. Salas, B. R. Zutta, W. Buermann, S. L. Lewis, S. Hagen, S. Petrova, L. White, M. Silman, A. Morel, Benchmark map of forest carbon stocks in tropical regions across three continents. *Proc. Natl. Acad. Sci. U.S.A.* **108**, 9899–9904 (2011).
3. Y. Y. Liu, A. I. J. M. van Dijk, R. A. M. de Jeu, J. G. Canadell, M. F. McCabe, J. P. Evans, G. Wang, Recent reversal in loss of global terrestrial biomass. *Nat. Clim. Chang.* **5**, 470–474 (2015).
4. R. J. Keenan, G. A. Reams, F. Achard, J. V. de Freitas, A. Grainger, E. Lindquist, Dynamics of global forest area: Results from the FAO Global Forest Resources Assessment 2015. *For. Ecol. Manag.* **352**, 9–20 (2015).
5. J. A. Foley, R. De Fries, G. P. Asner, C. Barford, G. Bonan, S. R. Carpenter, F. S. Chapin, M. T. Coe, G. C. Daily, H. K. Gibbs, J. H. Helkowski, T. Holloway, E. A. Howard, C. J. Kucharik, C. Monfreda, J. A. Patz, I. C. Prentice, N. Ramankutty, P. K. Snyder, Global consequences of land use. *Science* **309**, 570–574 (2005).
6. A. Baccini, W. Walker, L. Carvalho, M. Farina, D. Sulla-Menashe, R. A. Houghton, Tropical forests are a net carbon source based on aboveground measurements of gain and loss. *Science* **358**, 230–234 (2017).
7. L. B. Vedovato, M. G. Fonseca, E. Arai, L. O. Anderson, L. E. O. C. Aragão, The extent of 2014 forest fragmentation in the Brazilian Amazon. *Reg. Environ. Chang.* **16**, 2485–2490 (2016).
8. C. H. L. Silva Junior, L. E. O. C. Aragão, M. G. Fonseca, C. T. Almeida, L. B. Vedovato, L. O. Anderson, Deforestation-induced fragmentation increases forest fire occurrence in central Brazilian Amazonia. *Forests* **9**, 305 (2018).
9. L. V. Ferreira, W. F. Laurance, Effects of forest fragmentation on mortality and damage of selected trees in central Amazonia. *Conserv. Biol.* **11**, 797–801 (1997).
10. W. F. Laurance, S. G. Laurance, L. V. Ferreira, J. M. Rankin-de Merona, C. Gascon, T. E. Lovejoy, Biomass collapse in Amazonian forest fragments. *Science* **278**, 1117–1118 (1997).
11. H. E. M. Nascimento, W. F. Laurance, Biomass dynamics in Amazonian forest fragments. *Ecol. Appl.* **14**, 127–138 (2004).
12. E. N. Broadbent, G. P. Asner, M. Keller, D. E. Knapp, P. J. C. Oliveira, J. N. Silva, Forest fragmentation and edge effects from deforestation and selective logging in the Brazilian Amazon. *Biol. Conserv.* **141**, 1745–1757 (2008).
13. D. Armenteras, T. M. González, J. Retana, Forest fragmentation and edge influence on fire occurrence and intensity under different management types in Amazon forests. *Biol. Conserv.* **159**, 73–79 (2013).
14. R. Chaplin-Kramer, I. Ramler, R. Sharp, N. M. Haddad, J. S. Gerber, P. C. West, L. Mandle, P. Engstrom, A. Baccini, S. Sim, C. Mueller, H. King, Degradation in carbon stocks near tropical forest edges. *Nat. Commun.* **6**, 10158 (2015).
15. D. Armenteras, J. S. Barreto, K. Tabor, R. Molowny-Horas, J. Retana, Changing patterns of fire occurrence in proximity to forest edges, roads and rivers between NW Amazonian countries. *Biogeosciences* **14**, 2755–2765 (2017).
16. F. Taubert, R. Fischer, J. Groeneveld, S. Lehmann, M. S. Müller, E. Rödig, T. Wiegand, A. Huth, Global patterns of tropical forest fragmentation. *Nature* **554**, 519–522 (2018).
17. K. Riitters, J. Wickham, R. O'Neill, B. Jones, E. Smith, Global-scale patterns of forest fragmentation. *Conserv. Ecol.* **4**, 3 (2000).
18. M. C. Hansen, L. Wang, X.-P. Song, A. Tyukavina, S. Turubanova, P. V. Potapov, S. V. Stehman, The fate of tropical forest fragments. *Sci. Adv.* **6**, eaax8574 (2020).
19. N. M. Haddad, L. A. Brudvig, J. Clobert, K. F. Davies, A. Gonzalez, R. D. Holt, T. E. Lovejoy, J. O. Sexton, M. P. Austin, C. D. Collins, W. M. Cook, E. I. Damschen, R. M. Ewers, B. L. Foster, C. N. Jenkins, A. J. King, W. F. Laurance, D. J. Levey, C. R. Margules, B. A. Melbourne, A. O. Nicholls, J. L. Orrock, D.-X. Song, J. R. Townshend, Habitat fragmentation and its lasting impact on Earth's ecosystems. *Sci. Adv.* **1**, e1500052 (2015).
20. UNFCCC - United Nations Framework Convention on Climate Change, Forest reference emission levels (2019); https://redd.unfccc.int/fact-sheets/forest-reference-emission-levels.html.
21. I. Numata, M. A. Cochrane, D. A. Roberts, J. V. Soares, C. M. Souza Jr., M. H. Sales, Biomass collapse and carbon emissions from forest fragmentation in the Brazilian Amazon. *J. Geophys. Res.* **115**, G03027 (2010).
22. L. de Barros Viana Hissa, H. Müller, A. P. D. Aguiar, P. Hostert, T. Lakes, Historical carbon fluxes in the expanding deforestation frontier of Southern Brazilian Amazonia (1985–2012). *Reg. Environ. Chang.* **18**, 77–89 (2018).
23. I. Numata, M. A. Cochrane, C. M. Souza Jr., M. H. Sales, Carbon emissions from deforestation and forest fragmentation in the Brazilian Amazon. *Environ. Res. Lett.* **6**, 044003 (2011).
24. S. Pütz, J. Groeneveld, K. Henle, C. Knogge, A. C. Martensen, M. Metz, J. P. Metzger, M. C. Ribeiro, M. Dantas de Paula, A. Huth, Long-term carbon loss in fragmented Neotropical forests. *Nat. Commun.* **5**, 5037 (2014).
25. K. Brinck, R. Fischer, J. Groeneveld, S. Lehmann, M. Dantas De Paula, S. Pütz, J. O. Sexton, D. Song, A. Huth, High resolution analysis of tropical forest fragmentation and its impact on the global carbon cycle. *Nat. Commun.* **8**, 14855 (2017).
26. S. L. Maxwell, T. Evans, J. E. M. Watson, A. Morel, H. Grantham, A. Duncan, N. Harris, P. Potapov, R. K. Runting, O. Venter, S. Wang, Y. Malhi, Degradation and forgone removals increase the carbon impact of intact forest loss by 626%. *Sci. Adv.* **5**, eaax2546 (2019).
27. D. R. A. Almeida, S. C. Stark, J. Schietti, J. L. C. Camargo, N. T. Amazonas, E. B. Gorgens, D. M. Rosa, M. N. Smith, R. Valbuena, S. Saleska, A. Andrade, R. Mesquita, S. G. Laurance, W. F. Laurance, T. E. Lovejoy, E. N. Broadbent, Y. E. Shimabukuro, G. G. Parker, M. Lefsky, C. A. Silva, P. H. S. Brancalion, Persistent effects of fragmentation on tropical rainforest canopy structure after 20 yr of isolation. *Ecol. Appl.* **29**, e01952 (2019).
28. M. C. Hansen, P. V. Potapov, R. Moore, M. Hancher, S. A. Turubanova, A. Tyukavina, D. Thau, S. V. Stehman, S. J. Goetz, T. R. Loveland, A. Kommareddy, A. Egorov, L. Chini, C. O. Justice, J. R. G. Townshend, High-resolution global maps of 21st-century forest cover change. *Science* **342**, 850–853 (2013).
29. M. Longo, M. Keller, M. N. dos-Santos, V. Leitold, E. R. Pinagé, A. Baccini, S. Saatchi, E. M. Nogueira, M. Batistella, D. C. Morton, Aboveground biomass variability across intact and degraded forests in the Brazilian Amazon. *Glob. Biogeochem. Cycles* **30**, 1639–1660 (2016).
30. M. A. Lefsky, W. B. Cohen, G. G. Parker, D. J. Harding, Lidar remote sensing for ecosystem studies. *Bioscience* **52**, 19–30 (2002).
31. E. M. Ordway, G. P. Asner, Carbon declines along tropical forest edges correspond to heterogeneous effects on canopy structure and function. *Proc. Natl. Acad. Sci. U.S.A.* **117**, 7863–7870 (2020).
32. M. Melito, J. P. Metzger, A. A. de Oliveira, Landscape-level effects on aboveground biomass of tropical forests: A conceptual framework. *Glob. Chang. Biol.* **24**, 597–607 (2018).
33. I. Numata, S. S. Silva, M. A. Cochrane, M. V. N. d'Oliveira, Fire and edge effects in a fragmented tropical forest landscape in the southwestern Amazon. *For. Ecol. Manag.* **401**, 135–146 (2017).
34. M. D. Velasco Gomez, R. Beuchle, Y. Shimabukuro, R. Grecchi, D. Simonetti, H. D. Eva, F. Achard, A long-term perspective on deforestation rates in the Brazilian Amazon. *ISPRS* **XL-7/W3**, 539–544 (2015).
35. Instituto Nacional de Pesquisas Espaciais (INPE), PRODES - Monitoramento da floresta amazônica brasileira por satélite (2020); http://www.obt.inpe.br/OBT/assuntos/programas/amazonia/prodes.
36. Ministério do Meio Ambiente (MMA), *Plano de Ação para prevenção e controle do desmatamento na Amazônia Legal (PPCDAm): 3ª fase (2012-2015) pelo uso sustentável e conservação da Floresta* (MMA, Brasíla, 2013); http://combateaodesmatamento.mma.gov.br/images/conteudo/PPCDAM_3aFase.pdf.
37. N. G. R. de Mello, P. Artaxo, Evolução do Plano de Ação para Prevenção e Controle do Desmatamento na Amazônia Legal. *Rev. do Inst. Estud. Bras.*, 108–129 (2017).
38. P. H. S. Brancalion, L. C. Garcia, R. Loyola, R. R. Rodrigues, V. D. Pillar, T. M. Lewinsohn, A critical analysis of the Native Vegetation Protection Law of Brazil (2012): Updates and ongoing initiatives. *Nat. Conserv.* **14**, 1–15 (2016).

39. J. Barlow, E. Berenguer, R. Carmenta, F. França, Clarifying Amazonia's burning crisis. *Glob. Chang. Biol.* **26**, 319–321 (2020).
40. Associação Nacional dos Servidores de Meio Ambiente (ASCEMA), Cronologia de um desastre anunciado: Ações do governo Bolsonaro para desmontar as políticas de meio ambiente no Brasil (2020); http://www.ascemanacional.org.br/wp-content/uploads/2020/09/Dossie_Meio-Ambiente_Governo-Bolsonaro_revisado_02-set-2020-1.pdf.
41. D. Nepstad, D. McGrath, C. Stickler, A. Alencar, A. Azevedo, B. Swette, T. Bezerra, M. DiGiano, J. Shimada, R. Seroa da Motta, E. Armijo, L. Castello, P. Brando, M. C. Hansen, M. McGrath-Horn, O. Carvalho, L. Hess, Slowing Amazon deforestation through public policy and interventions in beef and soy supply chains. *Science* **344**, 1118–1123 (2014).
42. V. López Acevedo, Ecuador: Rainforest under siege, in *The 21st Century Fight for the Amazon*, M. Ungar, Ed. (Springer International Publishing, Cham, 2018), pp. 93–113.
43. RAISG - Amazonian Network of Georeferenced Socio-Environmental Information, Deforestation in the Amazonia (1970–2013) (2015); https://www.amazoniasocioambiental.org/en/download/deforestation-in-the-amazonia-1970-2013-atlas/.
44. C. Dezécache, E. Faure, V. Gond, J.-M. Salles, G. Vieilledent, B. Hérault, Gold-rush in a forested El Dorado: Deforestation leakages and the need for regional cooperation. *Environ. Res. Lett.* **12**, 034013 (2017).
45. K. Delvoye, M. Parahoe, H. Libretto, Suriname: An exposed interior, in *The 21st Century Fight for the Amazon*, M. Ungar, Ed. (Springer International Publishing, Cham, 2018), pp. 149–170.
46. G. P. Asner, R. Tupayachi, Accelerated losses of protected forests from gold mining in the Peruvian Amazon. *Environ. Res. Lett.* **12**, 094004 (2016).
47. M. K. Steininger, C. J. Tucker, J. R. G. Townshend, T. J. Killeen, A. Desch, V. Bell, P. Ersts, Tropical deforestation in the Bolivian Amazon. *Environ. Conserv.* **28**, 127–134 (2001).
48. D. Armenteras, G. Rudas, N. Rodriguez, S. Sua, M. Romero, Patterns and causes of deforestation in the Colombian Amazon. *Ecol. Indic.* **6**, 353–368 (2006).
49. W. F. Laurance, J. L. C. Camargo, P. M. Fearnside, T. E. Lovejoy, G. B. Williamson, R. C. G. Mesquita, C. F. J. Meyer, P. E. D. Bobrowiec, S. G. W. Laurance, An Amazonian rainforest and its fragments as a laboratory of global change. *Biol. Rev.* **93**, 223–247 (2018).
50. I. Numata, M. A. Cochrane, D. A. Roberts, J. V. Soares, Determining dynamics of spatial and temporal structures of forest edges in South Western Amazonia. *For. Ecol. Manag.* **258**, 2547–2555 (2009).
51. W. F. Laurance, S. G. Laurance, P. Delamonica, Tropical forest fragmentation and greenhouse gas emissions. *For. Ecol. Manag.* **110**, 173–180 (1998).
52. M. Kalamandeen, E. Gloor, E. Mitchard, D. Quincey, G. Ziv, D. Spracklen, B. Spracklen, M. Adami, L. E. O. C. Aragão, D. Galbraith, Pervasive rise of small-scale deforestation in Amazonia. *Sci. Rep.* **8**, 1600 (2018).
53. W. F. Laurance, P. Delamônica, S. G. Laurance, H. L. Vasconcelos, T. E. Lovejoy, Rainforest fragmentation kills big trees. *Nature* **404**, 836 (2000).
54. P. M. Brando, J. K. Balch, D. C. Nepstad, D. C. Morton, F. E. Putz, M. T. Coe, D. Silverio, M. N. Macedo, E. A. Davidson, C. C. Nóbrega, A. Alencar, B. S. Soares-Filho, Abrupt increases in Amazonian tree mortality due to drought-fire interactions. *Proc. Natl. Acad. Sci. U.S.A.* **111**, 6347–6352 (2014).
55. V. Kapos, Effects of isolation on the water status of forest patches in the Brazilian Amazon. *J. Trop. Ecol.* **5**, 173–185 (1989).
56. J. L. C. Camargo, V. Kapos, Complex edge effects on soil moisture and microclimate in central Amazonian forest. *J. Trop. Ecol.* **11**, 205–221 (1995).
57. R. Trancoso, thesis, National Institute for Amazonian Research - INPA, Manaus (2008).
58. N. Sizer, E. V. J. Tanner, Responses of woody plant seedlings to edge formation in a lowland tropical rainforest, Amazonia. *Biol. Conserv.* **91**, 135–142 (1999).
59. T. E. Lovejoy, R. O. Bierregaard, A. B. Rylands, J. R. Malcom, C. E. Quintela, L. H. Harper, K. S. Brown Jr., A. H. Powell, G. V. N. Powell, H. O. R. Schubart, M. B. Hays, in *Conservation Biology: The Science of Scarcity and Diversity*, M. E. Soulé, Ed. (Sinauer Press, Massachusetts, 1986), pp. 257–285.
60. W. F. Laurance, L. V. Ferreira, J. M. Rankin-de Merona, S. G. Laurance, Rain forest fragmentation and the dynamics of Amazonian tree communities. *Ecology* **79**, 2032–2040 (1998).
61. R. K. Didham, J. H. Lawton, Edge structure determines the magnitude of changes in microclimate and vegetation structure in tropical forest fragments. *Biotropica* **31**, 17–30 (1999).
62. S. A. D'Angelo, A. C. S. Andrade, S. G. Laurance, W. F. Laurance, R. C. G. Mesquita, Inferred causes of tree mortality in fragmented and intact Amazonian forests. *J. Trop. Ecol.* **20**, 243–246 (2004).
63. W. F. Laurance, H. E. M. Nascimento, S. G. Laurance, A. C. Andrade, P. M. Fearnside, J. E. L. Ribeiro, R. L. Capretz, Rain forest fragmentation and the proliferation of successional trees. *Ecology* **87**, 469–482 (2006).
64. C. V. J. Silva, L. E. O. C. Aragão, J. Barlow, F. Espirito-Santo, P. J. Young, L. O. Anderson, E. Berenguer, I. Brasil, I. Foster Brown, B. Castro, R. Farias, J. Ferreira, F. França, P. M. L. A. Graça, L. Kirsten, A. P. Lopes, C. Salimon, M. A. Scaranello, M. Seixas, F. C. Souza, H. A. M. Xaud, Drought-induced Amazonian wildfires instigate a decadal-scale disruption of forest carbon dynamics. *Philos. Trans. R. Soc. B* **373**, 20180043 (2018).
65. C. H. L. Silva Junior, V. H. A. Heinrich, A. T. G. Freire, I. S. Broggio, T. M. Rosan, J. Doblas, L. O. Anderson, G. X. Rousseau, Y. E. Shimabukuro, C. A. Silva, J. I. House, L. E. O. C. Aragão, Benchmark maps of 33 years of secondary forest age for Brazil. *Sci. Data* **7**, 269 (2020).
66. R. C. G. Mesquita, P. Delamônica, W. F. Laurance, Effect of surrounding vegetation on edge-related tree mortality in Amazonian forest fragments. *Biol. Conserv.* **91**, 129–134 (1999).
67. M. A. Cochrane, Synergistic interactions between habitat fragmentation and fire in evergreen tropical forests. *Conserv. Biol.* **15**, 1515–1521 (2001).
68. M. A. Cochrane, W. F. Laurance, Fire as a large-scale edge effect in Amazonian forests. *J. Trop. Ecol.* **18**, 311–325 (2002).
69. M. A. Cochrane, W. F. Laurance, Synergisms among fire, land use, and climate change in the Amazon. *AMBIO* **37**, 522–527 (2008).
70. A. Cano-Crespo, P. J. C. Oliveira, A. Boit, M. Cardoso, K. Thonicke, Forest edge burning in the Brazilian Amazon promoted by escaping fires from managed pastures. *J. Geophys. Res. Biogeosci.* **120**, 2095–2107 (2015).
71. L. E. O. C. Aragão, Y. Malhi, N. Barbier, A. Lima, Y. Shimabukuro, L. Anderson, S. Saatchi, Interactions between rainfall, deforestation and fires during recent years in the Brazilian Amazonia. *Philos. Trans. R. Soc. Lond. Ser. B Biol. Sci.* **363**, 1779–1785 (2008).
72. D. V. Silvério, P. M. Brando, M. M. C. Bustamante, F. E. Putz, D. M. Marra, S. R. Levick, S. E. Trumbore, Fire, fragmentation, and windstorms: A recipe for tropical forest degradation. *J. Ecol.* **107**, 656–667 (2019).
73. J. A. Marengo, C. M. Souza Jr., K. Thonicke, C. Burton, K. Halladay, R. A. Betts, L. M. Alves, W. R. Soares, Changes in climate and land use over the Amazon region: Current and future variability and trends. *Front. Earth Sci.* **6**, 228 (2018).
74. J. A. Marengo, J. C. Espinoza, Extreme seasonal droughts and floods in Amazonia: Causes, trends and impacts. *Int. J. Climatol.* **36**, 1033–1050 (2016).
75. R. J. W. Brienen, O. L. Phillips, T. R. Feldpausch, E. Gloor, T. R. Baker, J. Lloyd, G. Lopez-Gonzalez, A. Monteagudo-Mendoza, Y. Malhi, S. L. Lewis, R. Vásquez Martinez, M. Alexiades, E. Álvarez Dávila, P. Alvarez-Loayza, A. Andrade, L. E. O. C. Aragão, A. Araujo-Murakami, E. J. M. M. Arets, L. Arroyo, G. A. Aymard C, O. S. Bánki, C. Baraloto, J. Barroso, D. Bonal, R. G. A. Boot, J. L. C. Camargo, C. V. Castilho, V. Chama, K. J. Chao, J. Chave, J. A. Comiskey, F. Cornejo Valverde, L. da Costa, E. A. de Oliveira, A. Di Fiore, T. L. Erwin, S. Fauset, M. Forsthofer, D. R. Galbraith, E. S. Grahame, N. Groot, B. Hérault, N. Higuchi, E. N. Honorio Coronado, H. Keeling, T. J. Killeen, W. F. Laurance, S. Laurance, J. Licona, W. E. Magnussen, B. S. Marimon, B. H. Marimon-Junior, C. Mendoza, D. A. Neill, E. M. Nogueira, P. Núñez, N. C. Pallqui Camacho, A. Parada, G. Pardo-Molina, J. Peacock, M. Peña-Claros, G. C. Pickavance, N. C. A. Pitman, L. Poorter, A. Prieto, C. A. Quesada, F. Ramírez, H. Ramírez-Angulo, Z. Restrepo, A. Roopsind, A. Rudas, R. P. Salomão, M. Schwarz, N. Silva, J. E. Silva-Espejo, M. Silveira, J. Stropp, J. Talbot, H. ter Steege, J. Teran-Aguilar, J. Terborgh, R. Thomas-Caesar, M. Toledo, M. Torello-Raventos, R. K. Umetsu, G. M. F. van der Heijden, P. van der Hout, I. C. Guimarães Vieira, S. A. Vieira, E. Vilanova, V. A. Vos, R. J. Zagt, Long-term decline of the Amazon carbon sink. *Nature* **519**, 344–348 (2015).
76. L. E. O. C. Aragão, Y. Malhi, R. M. Roman-Cuesta, S. Saatchi, L. O. Anderson, Y. E. Shimabukuro, Spatial patterns and fire response of recent Amazonian droughts. *Geophys. Res. Lett.* **34**, L07701 (2007).
77. L. E. O. C. Aragão, L. O. Anderson, M. G. Fonseca, T. M. Rosan, L. B. Vedovato, F. H. Wagner, C. V. J. Silva, C. H. L. Silva Junior, E. Arai, A. P. Aguiar, J. Barlow, E. Berenguer, M. N. Deeter, L. G. Domingues, L. Gatti, M. Gloor, Y. Malhi, J. A. Marengo, J. B. Miller, O. L. Phillips, S. Saatchi, 21st century drought-related fires counteract the decline of Amazon deforestation carbon emissions. *Nat. Commun.* **9**, 536 (2018).
78. C. H. L. Silva Junior, L. O. Anderson, A. L. Silva, C. T. Almeida, R. Dalagnol, M. A. J. S. Pletsch, T. V. Penha, R. A. Paloschi, L. E. O. C. Aragão, Fire responses to the 2010 and 2015/2016 Amazonian droughts. *Front. Earth Sci.* **7**, 97 (2019).
79. UNFCCC - Framework Convention on Climate Change, The Paris Agreement (2015); https://unfccc.int/process-and-meetings/the-paris-agreement/the-paris-agreement.
80. IPCC - Intergovernmental Panel on Climate Change, Special Report on Global Warming of 1.5°C: Summary for Policymakers (2018); https://www.ipcc.ch/sr15/chapter/spm/.
81. V. Masson-Delmotte, P. Zhai, H.-O. Pörtner, D. Roberts, J. Skea, P. R. Shukla, A. Pirani, W. Moufouma-Okia, C. Péan, R. Pidcock, S. Connors, J. B. R. Matthews, Y. Chen, X. Zhou, M. I. Gomis, E. Lonnoy, T. Maycock, M. Tignor, T. Waterfield, *Global Warming of 1.5 °C: Summary for Policymakers* (World Meteorological Organization, 2018).
82. H. D. Eva, O. Huber, F. Achard, H. Balslev, S. Beck, H. Behling, A. S. Belward, R. Beuchle, A. Cleef, M. Colchester, J. Duivenvoorden, M. Hoogmoed, W. Junk, P. Kabat, B. Kruijt, Y. Malhi, J. M. Müller, J. M. Pereira, C. Peres, G. T. Prance, J. Roberts, J. Salo, *A Proposal for Defining the Geographical Boundaries of Amazonia* (Publications Office, Luxembourg, 2005).

83. J.-F. Pekel, A. Cottam, N. Gorelick, A. S. Belward, High-resolution mapping of global surface water and its long-term changes. *Nature* **540**, 418–422 (2016).
84. K. A. C. Gasparini, C. H. L. Silva Junior, Y. E. Shimabukuro, E. Arai, L. E. O. C. Aragão, C. A. Silva, P. L. Marshall, Determining a threshold to delimit the Amazonian Forests from the Tree Canopy Cover 2000 GFC Data. *Sensors* **19**, 5020 (2019).
85. P.-E. Danielsson, Euclidean distance mapping. *Comput. Graph. Image Process.* **14**, 227–248 (1980).
86. V. Leitold, M. Keller, D. C. Morton, B. D. Cook, Y. E. Shimabukuro, Airborne lidar-based estimates of tropical forest structure in complex terrain: Opportunities and trade-offs for REDD+. *Carbon Balance Manag.* **10**, 3 (2015).
87. D. Kushary, Bootstrap methods and their application. *Technometrics* **42**, 216–217 (2000).
88. R Core Team, R: A language and environment for statistical computing. R Foundation for Statistical Computing, Vienna, Austria (2020); https://www.r-project.org.
89. J. Chave, C. Andalo, S. Brown, M. A. Cairns, J. Q. Chambers, D. Eamus, H. Fölster, F. Fromard, N. Higuchi, T. Kira, J.-P. Lescure, B. W. Nelson, H. Ogawa, H. Puig, B. Riéra, T. Yamakura, Tree allometry and improved estimation of carbon stocks and balance in tropical forests. *Oecologia* **145**, 87–99 (2005).
90. F. de Mendiburu, Package 'agricolae', in *Statistical Procedures for Agricultural Research* (2017), pp. 157.
91. A. D. Jassby, J. E. Cloern, Package 'wq' (2016), pp. 42.
92. M. G. Kendall, *Rank Correlation Methods* (Charles Griffin, London, 1975).
93. H. B. Mann, Nonparametric tests against trend. *Econometrica* **13**, 245–259 (1945).
94. P. K. Sen, Estimates of the regression coefficient based on Kendall's tau. *J. Am. Stat. Assoc.* **63**, 1379–1389 (1968).
95. T. P. Hettmansperger, J. W. McKean, *Robust Nonparametric Statistical Methods* (CRC Press, ed. 2, 2010).
96. W. J. Conover, *Practical Nonparametric Statistics* (John Wiley & Sons, ed. 3, 1999).


**Acknowledgments:** This study is part of the Large-scale biosphere-atmosphere program in Amazonia (LBA). We thank the scientists at the University of Maryland (UMD), the Joint Research Centre (JRC), the Woods Hole Research Center (WHRC), and the National Institute for Space Research (INPE) for providing the freely available datasets. We also thank the Sustainable Landscapes Brazil project, supported by the Brazilian Agricultural Research Corporation (EMBRAPA), the United States Forest Service (USFS), the United States Agency for International Development (USAID), and the United States Department of State (DOS) that provided the LiDAR data. Last, we thank the editor and reviewers whose helpful comments and suggestions consistently helped to improve the clarity and robustness of this manuscript. **Funding:** This study was financed in part by the Coordenação de Aperfeiçoamento de Pessoal de Nível Superior - Brasil (CAPES) - Finance Code 001. L.E.O.C.A. was funded by the National Council for Scientific and Technological Development, CNPq (305054/2016-3) and the São Paulo Research Foundation, FAPESP (2016/02018-2). L.O.A. acknowledges funding from the Inter-American Institute for Global Change Research, IAI (SGP-HW 016), CNPq (442650/2018-3 and 309247/2016-0), and FAPESP (2016/02018-2). E.E.M. acknowledges funding from the Academy of Finland (decision numbers 318252 and 319905). The research carried out at the Jet Propulsion Laboratory, California Institute of Technology, was under a contract with the NASA. M.L. was supported by the NASA Postdoctoral Program, administered by Universities Space Research Association under contract with NASA. The funders had no role in study design, data collection and analysis, decision to publish, or preparation of the manuscript. **Author contributions:** C.H.L.S.J., L.E.O.C.A., and L.O.A contributed to the conception and design of the study. C.H.L.S.J. organized and processed the dataset. C.H.L.S.J. performed the statistical analysis. C.H.L.S.J. and L.E.O.C.A wrote the manuscript. L.O.A., M.G.F., Y.E.S., C.V., F.A., R.B., M.L., I.N., C.A.S., E.E.M., and S.S.S. contributed with the discussion of the results and with inputs to the manuscript. All authors approved the submitted manuscript version. **Competing interests:** The authors declare that they have no competing interests. **Data and materials availability:** The data that support the findings of this study are all publicly available from their sources. Processed data, products, and code produced in this study are available from the corresponding author upon reasonable request.

Submitted 5 February 2020
Accepted 17 August 2020
Published 30 September 2020
10.1126/sciadv.aaz8360

**Citation:** C. H. L. Silva Junior, L. E. O. C. Aragão, L. O. Anderson, M. G. Fonseca, Y. E. Shimabukuro, C. Vancutsem, F. Achard, R. Beuchle, I. Numata, C. A. Silva, E. E. Maeda, M. Longo, S. S. Saatchi, Persistent collapse of biomass in Amazonian forest edges following deforestation leads to unaccounted carbon losses. *Sci. Adv.* **6**, eaaz8360 (2020).

Science Advances

# Persistent collapse of biomass in Amazonian forest edges following deforestation leads to unaccounted carbon losses

Celso H. L. Silva Junior, Luiz E. O. C. Aragão, Liana O. Anderson, Marisa G. Fonseca, Yosio E. Shimabukuro, Christelle Vancutsem, Frédéric Achard, René Beuchle, Izaya Numata, Carlos A. Silva, Eduardo E. Maeda, Marcos Longo and Sassan S. Saatchi

*Sci Adv* **6** (40), eaaz8360.
DOI: 10.1126/sciadv.aaz8360

Science Advances
AAAS

advances.sciencemag.org/cgi/content/full/6/40/eaaz8360/DC1

# Supplementary Materials for

## Persistent collapse of biomass in Amazonian forest edges following deforestation leads to unaccounted carbon losses

Celso H. L. Silva Junior*, Luiz E. O. C. Aragão, Liana O. Anderson, Marisa G. Fonseca, Yosio E. Shimabukuro, Christelle Vancutsem, Frédéric Achard, René Beuchle, Izaya Numata, Carlos A. Silva, Eduardo E. Maeda, Marcos Longo, Sassan S. Saatchi

*Corresponding author. Email: celsohlsj@gmail.com

Published 30 September 2020, *Sci. Adv.* **6**, eaaz8360 (2020)
DOI: 10.1126/sciadv.aaz8360

**This PDF file includes:**

**Supplementary Materials**
**Supplementary Materials for Results**

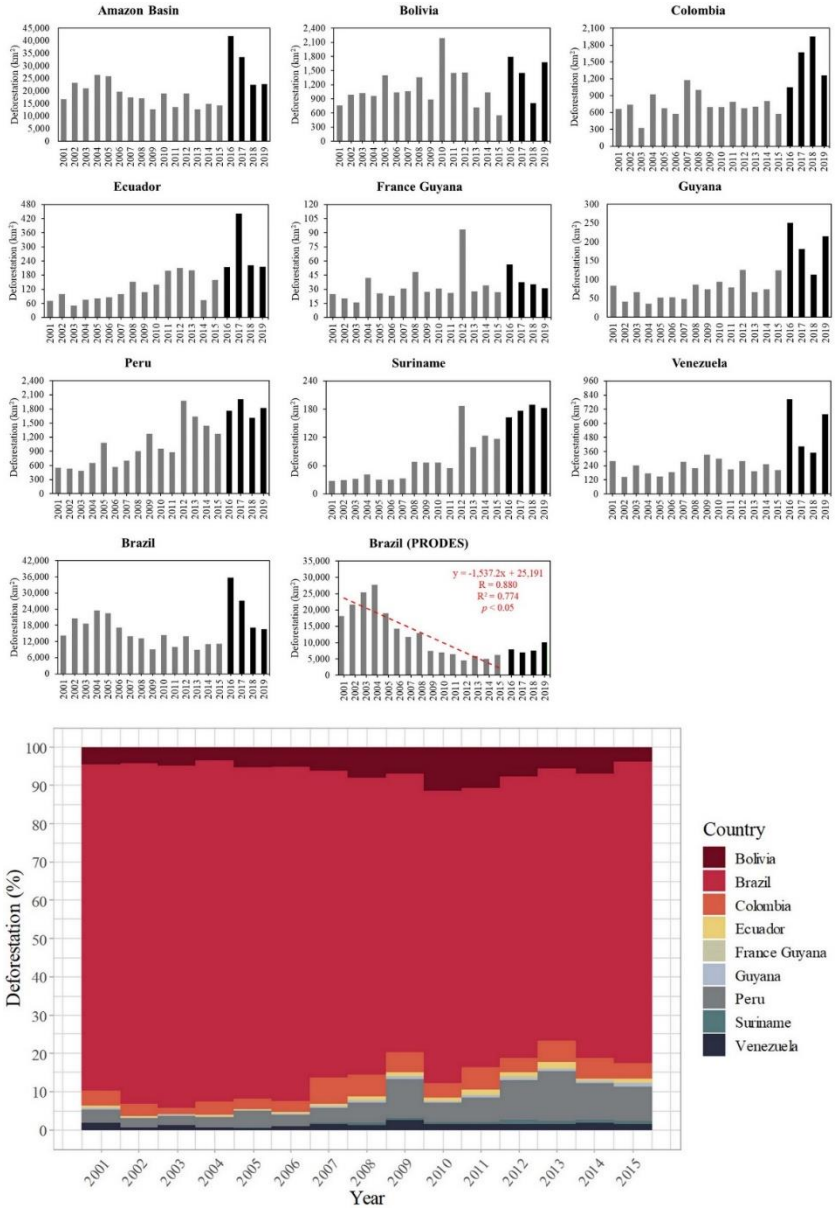


**Fig. S1. Annual deforestation rates in Amazonian countries, and their respective contributions (as percentage) to the total Amazonia deforestation.** Deforestation in the 2016-2019 period was measured from version 1.7 of the Global Forest Change dataset (GFC; https://earthenginepartners.appspot.com/science-2013-global-forest/download_v1.7.html). The Brazilian Amazon official deforestation rates were obtained from PRODES program (The Brazilian Amazon Deforestation Monitoring Program; http://terrabrasilis.dpi.inpe.br/en/home-page). After 2015, the difference between magnitudes of forest cover losses of GFC and PRODES data was due to the increase in drought-induced forest fires in the late 2015 and early 2016 *(85, 86)* that were detected by the GFC and not detected by PRODES (responsible for mapping the clear-cut deforestation in the Brazilian Amazon).

**Table S1. Relative deforested area for each Amazonian country during the 2001-2015 period.** The relative deforested area was calculated in relation to the Amazonia country area. SD is the standard deviation.

| Country | Area ($km^2$) | Year | | | | | | | | | | | | | | | |
|---|---|---|---|---|---|---|---|---|---|---|---|---|---|---|---|---|---|
| | | Relative Deforestation Area (%) | | | | | | | | | | | | | | | |
| | | 2001 | 2002 | 2003 | 2004 | 2005 | 2006 | 2007 | 2008 | 2009 | 2010 | 2011 | 2012 | 2013 | 2014 | 2015 | Mean±SD |
| Bolivia | 430,357 | 0.178 | 0.230 | 0.238 | 0.223 | 0.325 | 0.241 | 0.246 | 0.316 | 0.207 | 0.508 | 0.337 | 0.340 | 0.167 | 0.242 | 0.128 | 0.262±0.090 |
| Brazil | 4,182,580 | 0.341 | 0.493 | 0.447 | 0.561 | 0.536 | 0.411 | 0.334 | 0.315 | 0.219 | 0.345 | 0.238 | 0.334 | 0.214 | 0.264 | 0.267 | 0.355±0.109 |
| Colombia | 476,532 | 0.139 | 0.156 | 0.067 | 0.194 | 0.141 | 0.120 | 0.247 | 0.210 | 0.146 | 0.147 | 0.166 | 0.141 | 0.148 | 0.169 | 0.120 | 0.154±0.040 |
| Ecuador | 74,354 | 0.095 | 0.133 | 0.067 | 0.103 | 0.108 | 0.116 | 0.133 | 0.204 | 0.145 | 0.188 | 0.266 | 0.282 | 0.268 | 0.100 | 0.216 | 0.162±0.068 |
| France Guyana | 83,420 | 0.030 | 0.024 | 0.019 | 0.050 | 0.031 | 0.028 | 0.037 | 0.058 | 0.033 | 0.037 | 0.031 | 0.112 | 0.033 | 0.041 | 0.032 | 0.040±0.021 |
| Guyana | 209,794 | 0.040 | 0.020 | 0.032 | 0.017 | 0.024 | 0.025 | 0.023 | 0.041 | 0.035 | 0.045 | 0.038 | 0.060 | 0.032 | 0.035 | 0.059 | 0.035±0.012 |
| Peru | 626,648 | 0.088 | 0.085 | 0.077 | 0.104 | 0.173 | 0.090 | 0.112 | 0.144 | 0.203 | 0.153 | 0.140 | 0.315 | 0.262 | 0.230 | 0.204 | 0.159±0.069 |
| Suriname | 145,977 | 0.019 | 0.020 | 0.022 | 0.028 | 0.021 | 0.021 | 0.022 | 0.047 | 0.046 | 0.046 | 0.037 | 0.128 | 0.068 | 0.085 | 0.080 | 0.046±0.031 |
| Venezuela | 444,246 | 0.063 | 0.032 | 0.055 | 0.039 | 0.033 | 0.042 | 0.062 | 0.049 | 0.075 | 0.068 | 0.047 | 0.063 | 0.043 | 0.057 | 0.045 | 0.052±0.013 |
| Amazonia | 6,673,908 | 0.251 | 0.348 | 0.314 | 0.395 | 0.389 | 0.296 | 0.261 | 0.255 | 0.189 | 0.283 | 0.204 | 0.285 | 0.188 | 0.223 | 0.213 | 0.273±0.065 |

**Table S2. Temporal trends of deforestation rates for each Amazonian country.** Where S is the Man-Kendall statistics and SD the standard deviation. The S statistic with an asterisk (*) means a significant temporal trend at 95% of significance level ($p \leq 0.05$).

| Country | S | Sen's Slope ($km^2$ $year^{-1}$) | Average±SD ($km^2$ $year^{-1}$) |
|---|---|---|---|
| Bolivia | 0.13 | 8.66 | 1,126±400 |
| Brazil | -0.55* | -773 | 14,835±4,706 |
| Colombia | 0.09 | 2.13 | 734±198 |
| Ecuador | 0.59* | 9.12 | 120±52 |
| France Guiana | 0.37 | 0.67 | 33±18 |
| Guyana | 0.45* | 3.71 | 73±27 |
| Peru | 0.67* | 67.97 | 994±450 |
| Suriname | 0.75* | 6.71 | 67±46 |
| Venezuela | 0.15 | 2.42 | 229±57 |

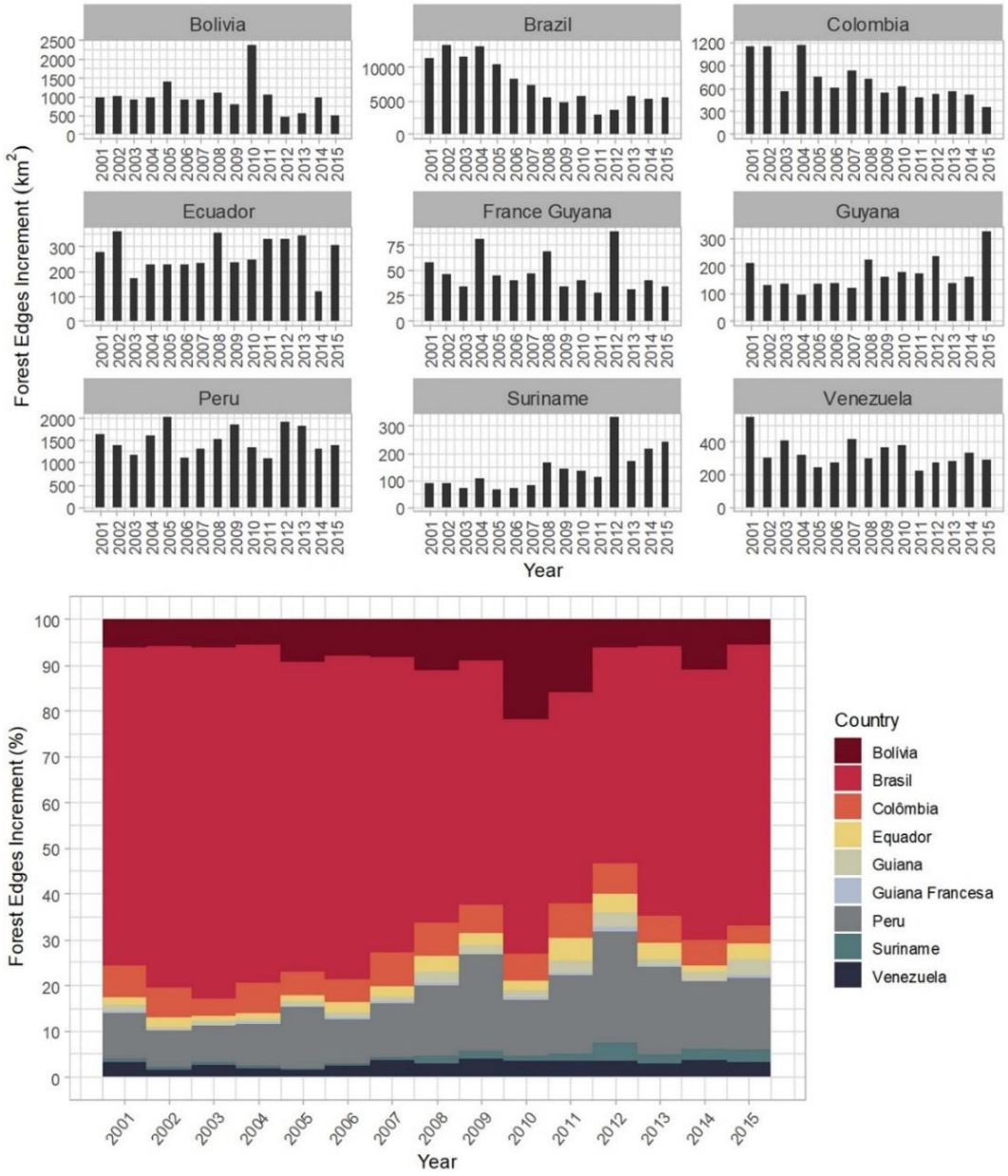


**Fig. S2. Annual rates of forest edges increment in Amazonian countries, and their respective contributions (as percentage) to the total Amazonia forest edge area.**

**Table S3. Temporal trends of forest edge increments for each Amazonian country.** Where S is the Man-Kendall statistics and SD the standard deviation. The S statistic with an asterisk (*) means a significant temporal trend at 95% of significance level ($p \leq 0.05$).

| Country | S | Sen Slope (km$^2$ year$^{-1}$) | Average±SD (km$^2$ year$^{-1}$) |
|---|---|---|---|
| Bolivia | -0.27 | -23 | 1000±455 |
| Brazil | -0.67* | -683 | 7600±3427 |
| Colombia | -0.65* | -49 | 705±261 |
| Ecuador | 0.17 | 4 | 266±72 |
| France Guiana | -0.29 | -1 | 171±59 |
| Guyana | 0.41* | 5 | 48±18 |
| Peru | -0.01 | -3 | 1510±300 |
| Suriname | 0.63* | 11 | 139±76 |
| Venezuela | -0.25 | -6 | 330±83 |

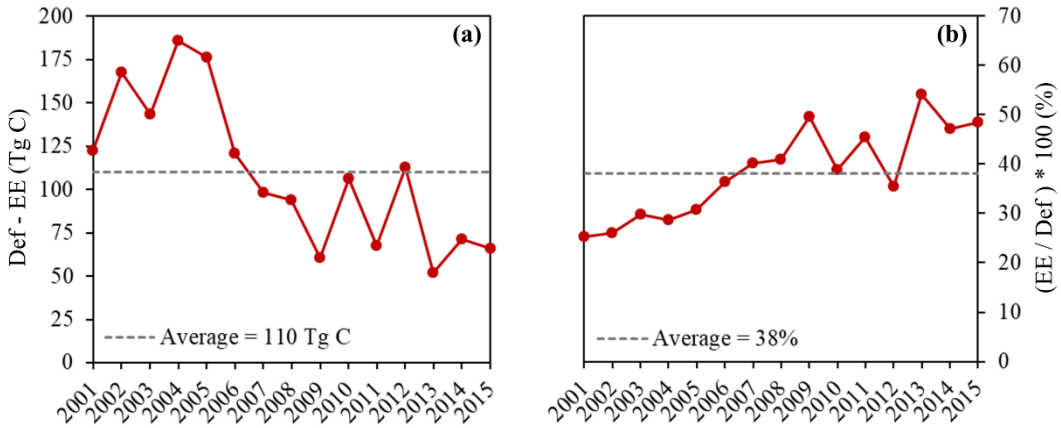


**Fig. S3. Comparison between the annual carbon losses from fragmentation and deforestation. (a)** Annual difference between carbon losses from deforestation and from fragmentation. **(b)** Annual proportion of carbon losses from edge effect in relation to carbon losses from deforestation (losses from edge effect divided by losses from deforestation). Where "Def" is Deforestation an "EE" is Edge Effect.

**Supplementary Materials for Discussion**

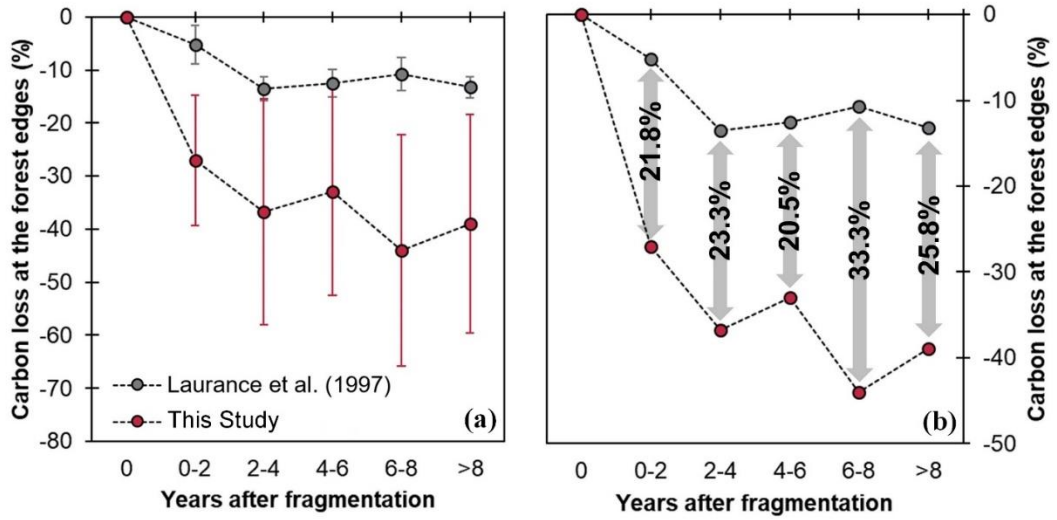


**Fig. S4. Comparison between carbon losses calculated in this study and those calculated by Laurance et al. (1997) (*10*). (a)** Carbon loss average subset by classes of years after edge formation. **(b)** Magnitude of the difference between methods. Vertical bars are the standard deviations.

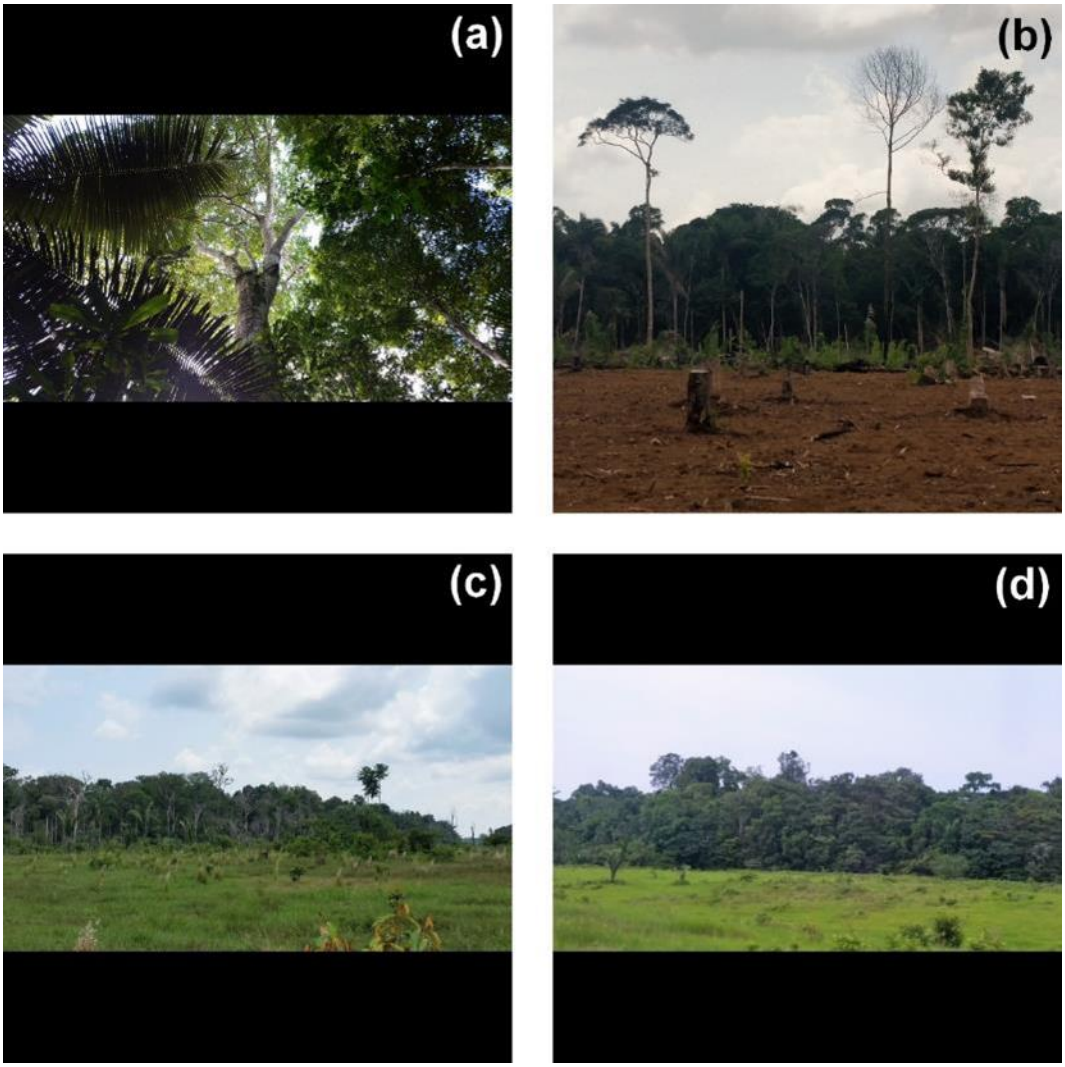


**Fig. S5. Photographic records taken in Autazes - AM, Central Brazilian Amazon, in November 2017. (a)** Example of the canopy of an intact forest area. **(b)** Example of new forest edge with a newly cleared area. **(c)** Example of a forest edge with apparent tree mortality. **(d)** An example of an old forest edge with apparent sealing by secondary vegetation. Photo Credit: Celso H. L. Silva Junior, National Institute for Space Research - INPE.

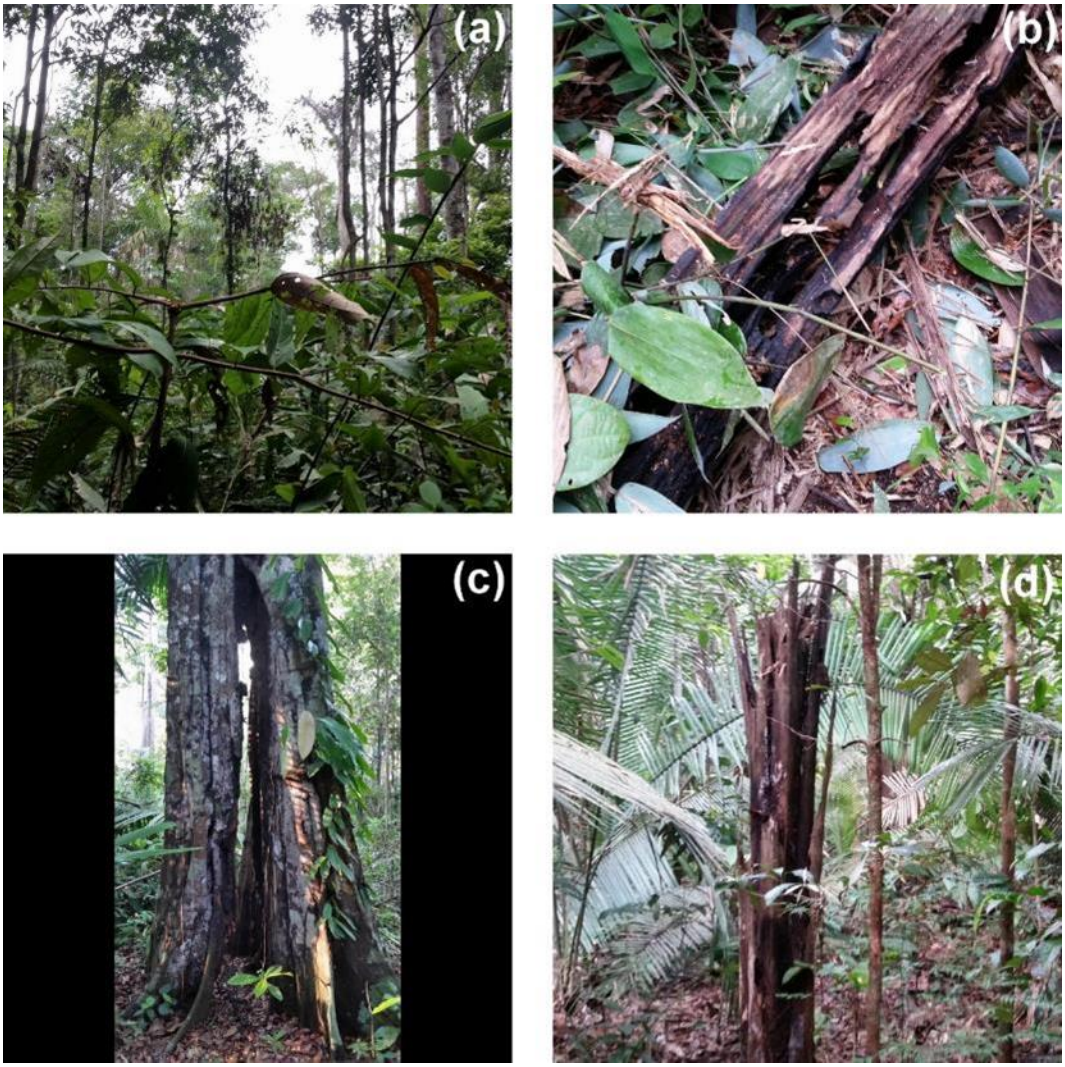


**Fig. S6. Photographic records taken in Autazes - AM, Central Brazilian Amazon, in November 2017. (a)** Example of a forest degraded by fire. **(b)** Fallen tree killed by fire. **(c)** Tree still alive with fire scars. **(d)** Palm tree standing dead by fire. Photo Credit: Celso H. L. Silva Junior, National Institute for Space Research - INPE.

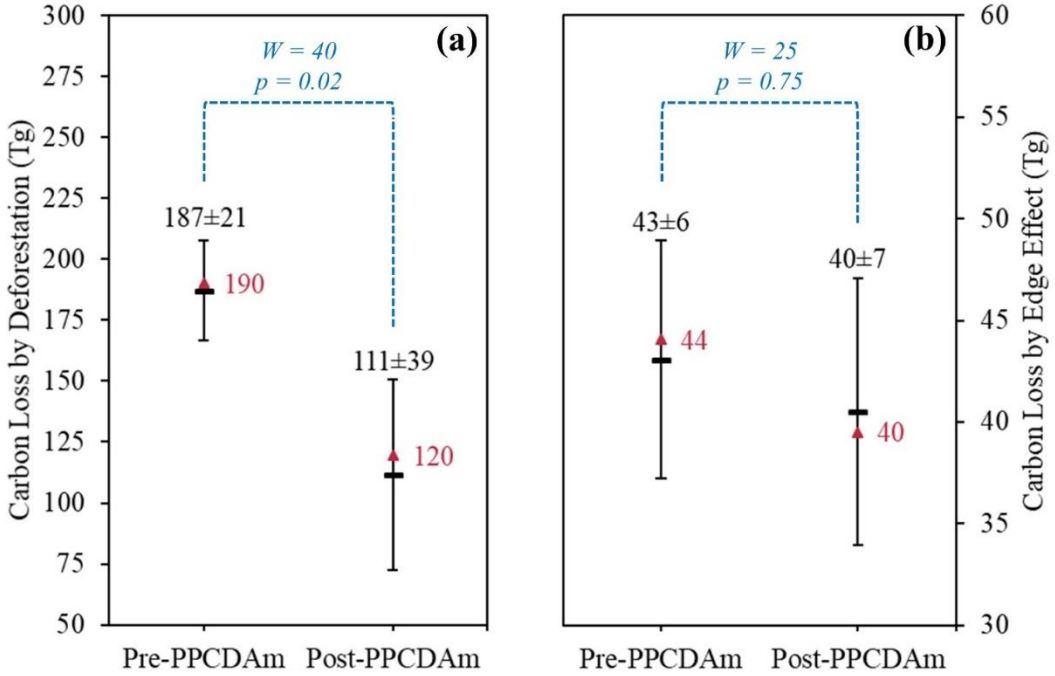


**Fig. S7. Comparison between carbon losses from deforestation and edge effect before (between 2001 and 2004) and after (between 2005 and 2015) the creation of PPCDAm** (*36*) **(Action Plan for Prevention and Control of Deforestation in Legal Amazon) in the Brazilian Amazon. (a)** Losses from deforestation. **(b)** Losses from edge effect. The horizontal black line is the average, the red triangle is the median, the black vertical line is the standard deviation, and in blue the values of the statistic (*W*) and p-value (*p*) of the Wilcoxon statistical test.

**Supplementary Materials for Materials and Methods**

**Forest cover mapping**

We produced 16 annual forest cover maps from 2000 to 2015 with 30-m spatial resolution for Amazonia. The maps included old-growth forests, secondary forests (before 2000) and planted forests. We adopted the delimitation of the Amazonia *sensu latissimo* proposed by Eva et al. (*82*), excluding the Andes and Planalto regions. This limit encompasses an area of 6,673,908 $km^2$, including areas from Brazil, Bolivia, Peru, Ecuador, Colombia, Venezuela, Guyana, Suriname, and French Guiana. All nine countries together host 95% of the remaining Amazonian old-growth forests (*82*).

To produce the forest cover maps, we used version 1.3 of the Global Forest Change dataset (https://earthenginepartners.appspot.com/science-2013-global-forest/download_v1.3.html) (*28*), which includes three products: (i) tree canopy cover (2000), (ii) forest cover loss (2001-2015) and (iii) forest cover gain (2000-2012) data. We also used the maximum water extent data (1984-2015) (https://global-surface-water.appspot.com) (*83*). All the data mentioned above are made available at 30-m spatial resolution. The temporal coverage of the datasets comprehends the Pre-PPCDAm (between 2001 and 2004) and Post-PPCDAm (between 2005 and 2015) period, implemented in the Brazilian Amazon for curbing illegal deforestation.

Initially, to produce the year 2000 forest map baseline, we applied the threshold of 80% tree canopy cover (Fig. S8a) for defining the old-growth forest area, as suggested by Gasparini et al. (*84*) (Fig. S8b). This threshold avoids the inclusion of non-forest formations (e.g., savannas) in Forest class (*84*). The forest class, hence, included all pixels with a percentage of tree canopy cover equal or greater than 80%, and as Non-forest class all pixels with a tree canopy cover percentage of less than 80%. Subsequently, we removed all pixels with forest cover gain between 2000 and 2012 (Fig. S8c). This procedure allowed the removal all secondary forest pixels start regrowing between 2000 and 2012. Wetland forests were also removed by intersecting the forest cover map with the map of flooded areas between 1984 and 2015 (Fig. S8d).

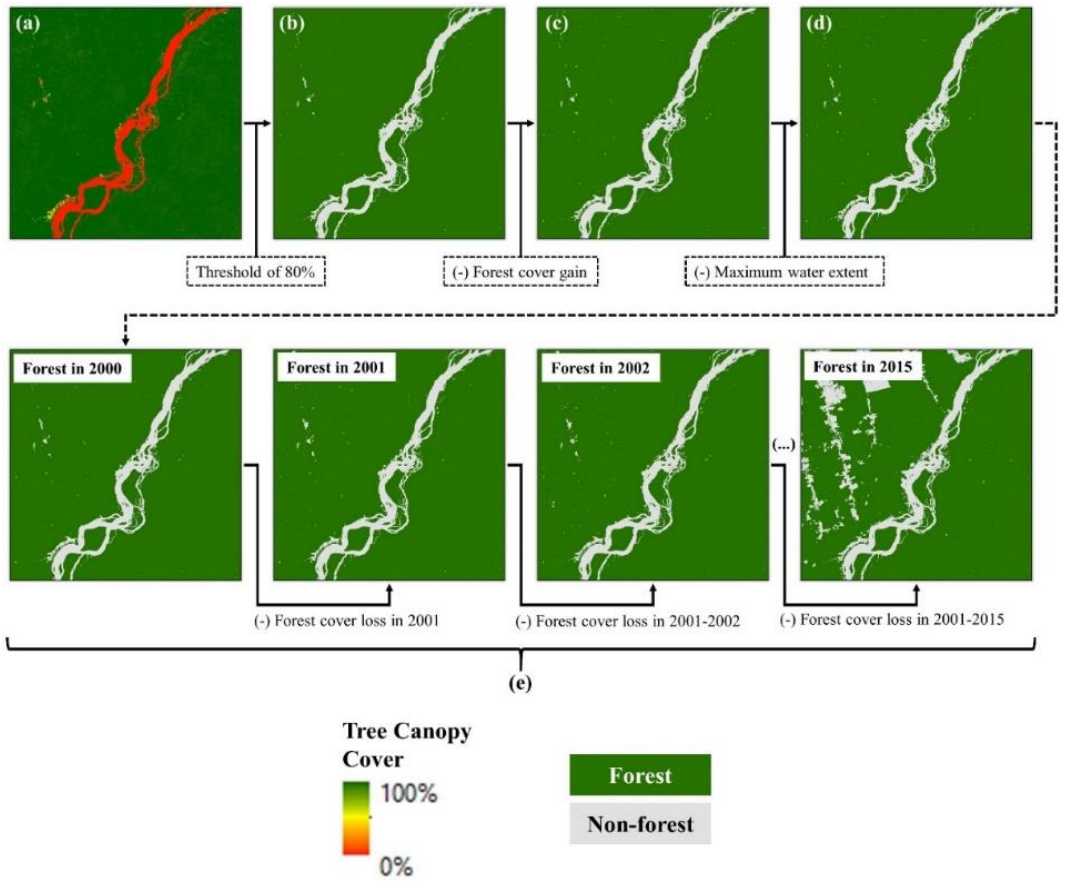


**Fig. S8. Forest cover mapping methods. (a)** Tree canopy cover data 2000. **(b)** Forest cover map 2000. **(c)** Forest cover map 2000 excluding the forest cover gain. (d) Forest cover map 2000 excluding the forest cover gain and maximum water extent. **(e)** Reconstruction of forest cover maps between 2001 and 2015.

Then, to obtain the forest maps (2001-2015), we removed year by year pixels with forest cover loss between 2001 and 2015 from the 2000 forest map, by using Boolean logic using the two sets of maps (Fig. S8e). For instance, to obtain the 2001 forest map using this procedure, all pixels with forest cover loss in 2001 were removed from the 2000 forest map. This procedure was repeated across all years (2001-2015).

Finally, to avoid the effect of isolated single pixels, for both Forest and Non-forest classes, we applied a move window filter for all annual forest maps (16 maps in total). We adopted the Sieve algorithm (https://www.gdal.org/gdal_sieve.html) from the Geospatial Data Abstraction Library – GDAL (https://www.gdal.org). The GDAL Sieve algorithm removes pixels smaller than a provided threshold (give in pixels) and replaces them with the pixel of neighbour value. Here we used the five-pixel threshold, which includes patches greater than four pixels (0.0036 $km^2$ or 0.36 ha).

**Identification of forest edges and quantification of age structure**

Using the forest cover maps (Fig. S9a), we produced 16 forest edges maps (2000 to 2015). For this study, we adopt a 100-m as the edge width, assuming the most significant AGC stocks loss typically occur within this distance in Amazonia (*10*, *33*). However, due to the spatial resolution (30-m) of our data, we considered for our analyses a width of 120 m, equivalent to four pixels, to define the forest edges. Initially, we attributed a null value for each pixel corresponding to the Forest class for the 16 forest cover maps (Fig. S9b). Subsequently, all pixels with the null value were filled with the Euclidean distance value (*85*) calculated from the Non-forest class (Fig. S9c). Finally, the calculated Euclidean distance was used to classify the pixels based on distance intervals, using three classes: Non-forest class (equal to 0m), Forest class (greater than 120m) and Forest-edge class (between 30 and 120m) (Fig. S9d).

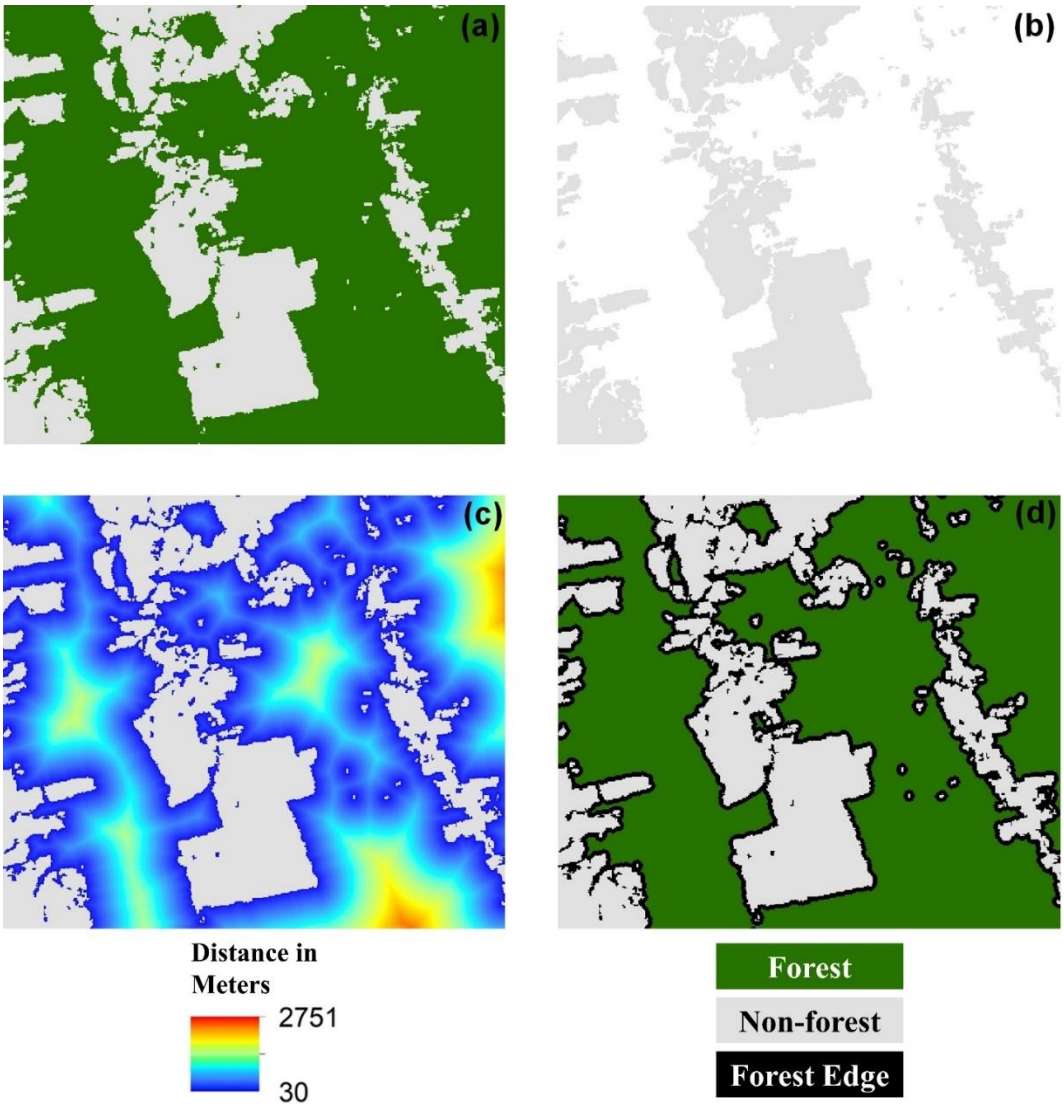


**Fig. S9. Workflow for forest edges mapping. (a)** Forest map. **(b)** Non-forest map. **(c)** Euclidian distance from non-forest areas. **(d)** Map of forest, non-forest, and forest edges.

Using the forest edges maps, we produced 15 forest edges age maps (2001 to 2015). Firstly, we removed from the forest edges maps (2001 to 2015) all the edges in 2000, which had an area of 416,793 km$^2$ (6.25% of Amazonia territory), because of the impossibility of estimating the age of forest edges in the year 2000. This first step also removed all natural forest edges formed at the boundaries between forest-water and forest-savannas, which were not of interest for our study. Then, we transform the forest edges maps into binary maps, where we assign the value of "1" to the forest edge class and "0" to the forest and Non-forest classes. Finally, we use the map algebra method to calculate the forest edges age, by summing the binary maps year by year cumulatively. From this procedure we obtained binary maps from 2001 to 2015, with the 2001 age map having only forest edges with one year old and the 2015 map having edges ranging from 1 to 15 years old (Fig. S10).

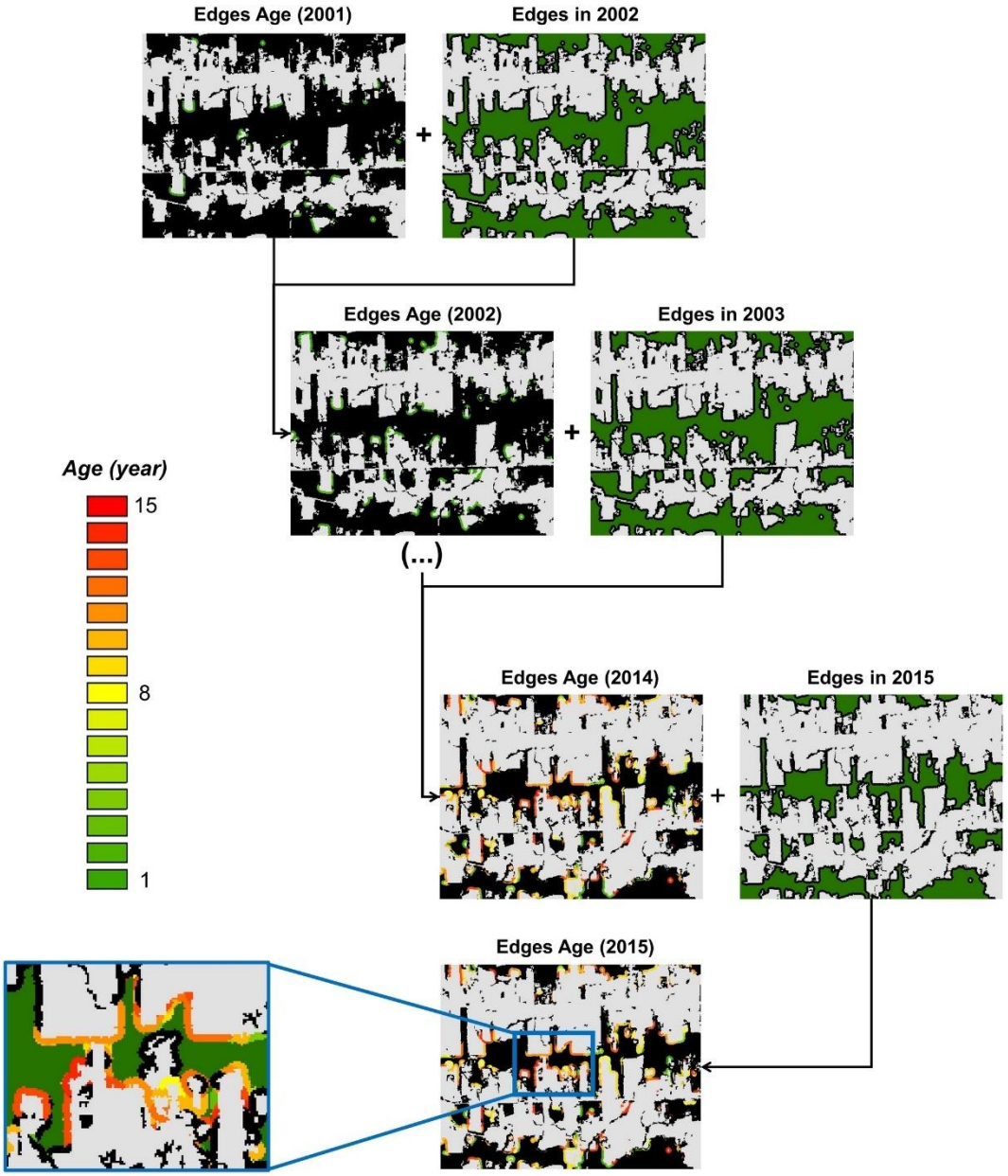


**Fig. S10. Workflow for the approach used for calculating forest edges age.**

**Carbon stock mapping from LiDAR data**

We produced 20 carbon maps with 50m spatial resolution, using a multitemporal LiDAR point clouds dataset, collected in 13 flight lines within the Brazilian Amazon (Fig. S11 and Table S4). The LiDAR data were obtained from the Sustainable Landscapes Project (https://www.paisagenslidar.cnptia.embrapa.br), which were collected using a LiDAR Airborne System with flights carried out between 2012 and 2015, totalling an area of 153.17 km$^2$. All the LiDAR plots have a point density higher than four points per squared meters (*86*) (Table S4).

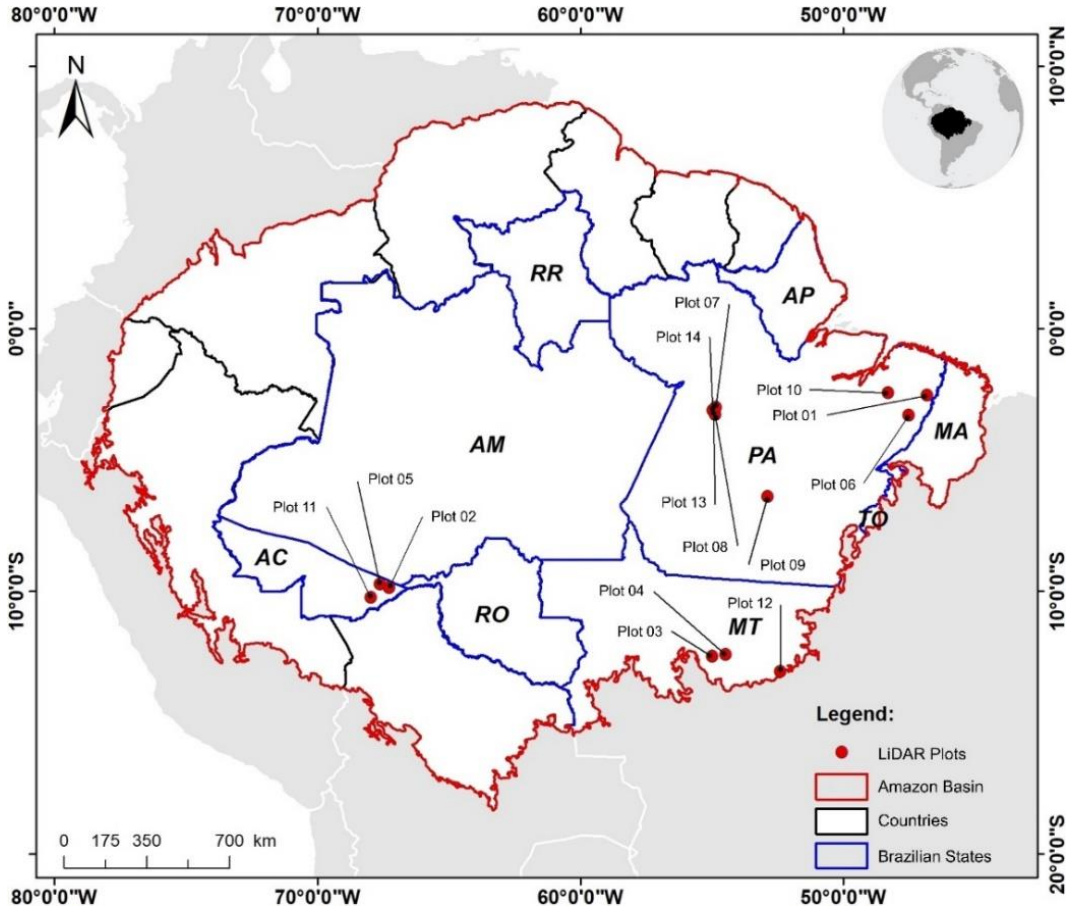


**Fig. S11. Spatial distribution of the LiDAR flight lines in Amazonia.** Brazilian States: AC, Acre; AM, Amazonas; AP, Amapá; MA, Maranhão; MT, Mato Grosso; PA, Pará; RO, Rondônia; RR, Roraima; TO, Tocantins.

**Table S4. Technical specifications of the instrument, aircraft and data collection settings for the LiDAR flight lines.**

| LiDAR Plots | Year of Acquisition | Average Return Density (points $m^{-2}$) | Average Density of First Return (points $m^{-2}$) | Average Flight Altitude (m) | Field of View (degree) |
|---|---|---|---|---|---|
| Plot 1 | 2013 | 16.80 | 9.30 | 853.40m | 11.00 |
| Plot 1 | 2014 | 38.20 | 17.20 | 853.40m | 11.00 |
| Plot 2 | 2013 | 33.39 | 15.57 | 900.00m | 11.10 |
| Plot 3 | 2013 | 38.34 | 25.84 | 853.00m | 9.80 |
| Plot 4 | 2015 | 38.59 | 29.82 | 850.00m | 12.00 |
| Plot 5 | 2013 | 66.61 | 30.48 | 900.00m | 11.10 |
| Plot 6 | 2013 | 11.78 | 6.58 | 853.40m | 11.00 |
| Plot 6 | 2014 | 40.00 | 17.75 | 853.40m | 11.00 |
| Plot 7 | 2015 | 49.53 | 26.40 | 850.00m | 12.00 |
| Plot 8 | 2015 | 58.67 | 29.16 | 850.00m | 12.00 |
| Plot 9 | 2012 | 30.10 | 20.40 | 850.00m | 11.00 |
| Plot 10 | 2013 | 24.25 | 15.14 | 853.40m | 9.80 |
| Plot 11 | 2014 | 40.70 | 18.40 | 900.00m | 11.10 |
| Plot 11 | 2013 | 10.80 | 5.20 | 900.00m | 11.10 |
| Plot 12 | 2012 | 13.70 | 7.05 | 850.00m | 11.00 |
| Plot 12 | 2014 | 41.05 | 16.70 | 853.00m | 10.00 |
| Plot 13 | 2012 | 36.90 | 23.11 | 850.00m | 11.10 |
| Plot 13 | 2013 | 29.95 | 17.12 | 853.40m | 11.00 |
| Plot 14 | 2012 | 38.90 | 23.90 | 850.00m | 11.10 |
| Plot 14 | 2013 | 29.95 | 17.12 | 853.40m | 11.00 |

We performed all LiDAR point clouds data processing in the FUSION 3.60 software (http://forsys.cfr.washington.edu/fusion/fusionlatest.html). Initially, we filtered the points classified as terrain for each LiDAR plot. Then, from the previously filtered points, we created Digital Terrain Models - DTM with 1-m spatial resolution (Fig. S12a). Subsequently, we normalised (altitude-to-height conversion) all points classified as vegetation using the DTM, to create for each flight line a Canopy Height Model - CHM with -m spatial resolution (Fig. S12b).

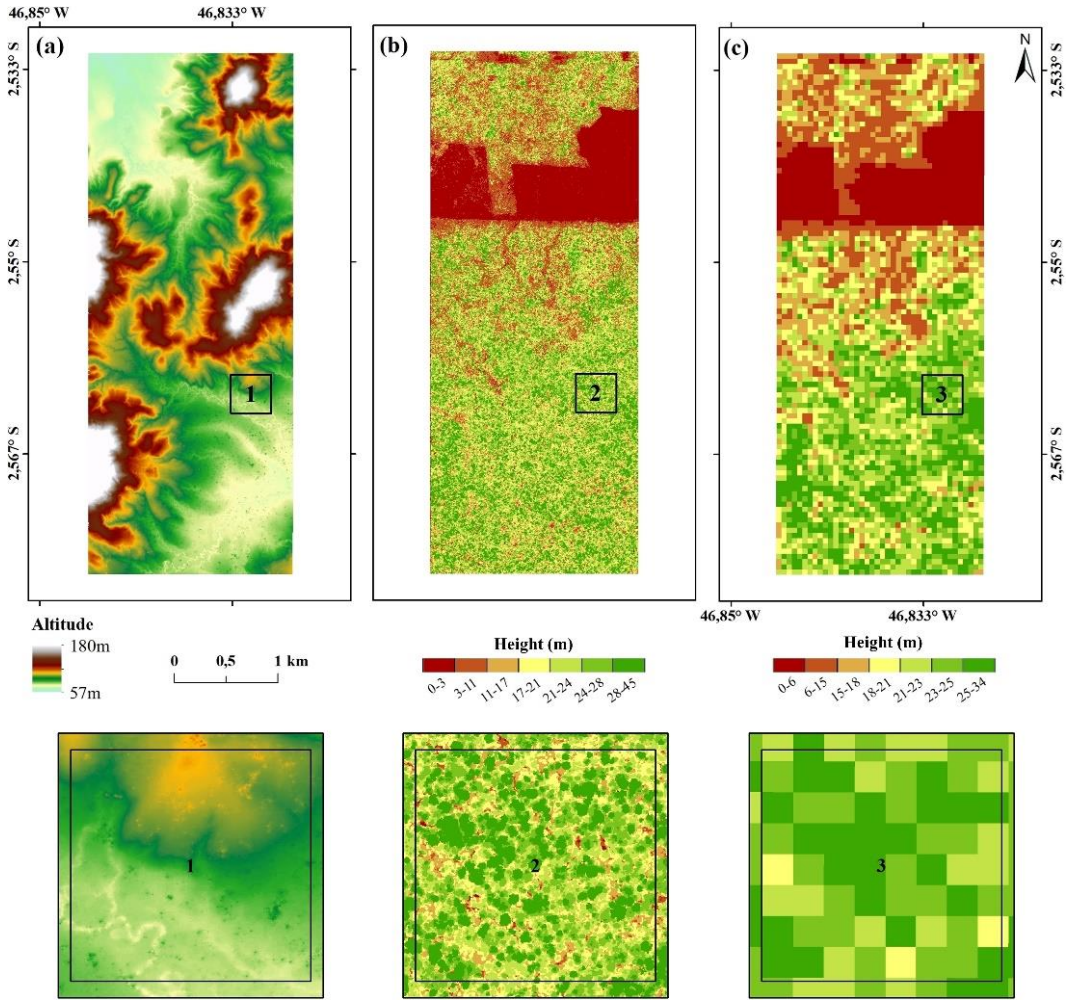


**Fig. S12. Products derived from LiDAR point clouds. (a)** Digital Terrain Model with 1m of spatial resolution. **(b)** Canopy Height Model with 1m of spatial resolution. **(c)** Canopy Height Model resampled to 50m of spatial resolution.

We used the methodology proposed by Longo et al. (*29*) to calculate above-ground forest carbon (for living trees) using the LiDAR data. To apply this method, we first created a 50-m spatial resolution CHM, using the average of the canopy heights at 1 m of spatial resolution (Fig. S12c). Then, we applied Equation 1 (*29*) for each 50-m of spatial resolution pixel in the CHM map.

$$C_{Stock} = 0.025 \cdot CHM_{50m}^{1.99} \qquad (1)$$

where $C_{Stock}$ is the carbon stock of each pixel in kg $m^{-2}$ (subsequently converted to Mg $ha^{-1}$, multiplying the result by 10), and $CHM_{50m}$ is the pixel value at 50m of spatial resolution in the Canopy Height Model (CHM). This equation had an adjusted $R^2$ of 0.68 and a Mean Square Error of 4.33 kg C $m^{-2}$ (*29*).

**Carbon stock loss model by edge effect and deforestation**

We use LiDAR carbon stock and forest edges age maps to model the carbon loss in forest edges as a function of edges age. Firstly, we overlaid the carbon stock map, of each LIDAR flight line, on the forest edge map to extract the carbon values for pixels in the forest edge and interior classes. For this approach, we considered the LiDAR collected at the same year as their respective forest edges age map. Then, we calculated the carbon average for the forest interior, which was consider as control areas, not impacted by edge effects (*10*, *33*). We also calculated the carbon average for the forest edges stratified by their respective ages. Finally, we calculated the percentage difference between the forest interior and forest edges AGC stocks for each age, leading to 152 samples of the carbon loss percentage for different edge ages.

Based on the conceptual model proposed by Melito et al. (*32*), we employed a non-linear rectangular hyperbolic regression (Michaelis-Menten kinetic equation, $R^2$=0.780) (Equation 2) using the average carbon loss stratified by forest edge ages (Fig. S13a). From a bootstrap approach (*87*), we calculate the 95% confidence intervals for all equation parameters based on 1000 random repetitions with replacement using the "boot" package (Package 'boot') implemented in the R statistical software (*88*) (version 3.4.4; https://www.r-project.org).

$$C_{Loss} = \frac{-42.815(\pm 2.966) \cdot E_{Age}}{0.836(\pm 0.411) + E_{Age}} + \varepsilon \qquad (2a)$$

$$Where\ \varepsilon \sim N(0, 5.767^2) \qquad (2b)$$

where $C_{Loss}$ is the carbon stock loss in percentage as a function of forest edge age, $E_{Age}$ is the edge age for the specific year, -42.815 is the value of the α parameter, and 0.836 is the value of the β parameter, ε is the estimated error for the equation, and 5.767 is the residual standard error. The values in parentheses were obtained through the 1000 bootstrap interactions process and represent the variation of each parameter, considering a 95% confidence interval. From the Equation 2a decay curve, we calculated the individual carbon loss percentage for each forest edge age (Fig. S13b and Tab. S5).

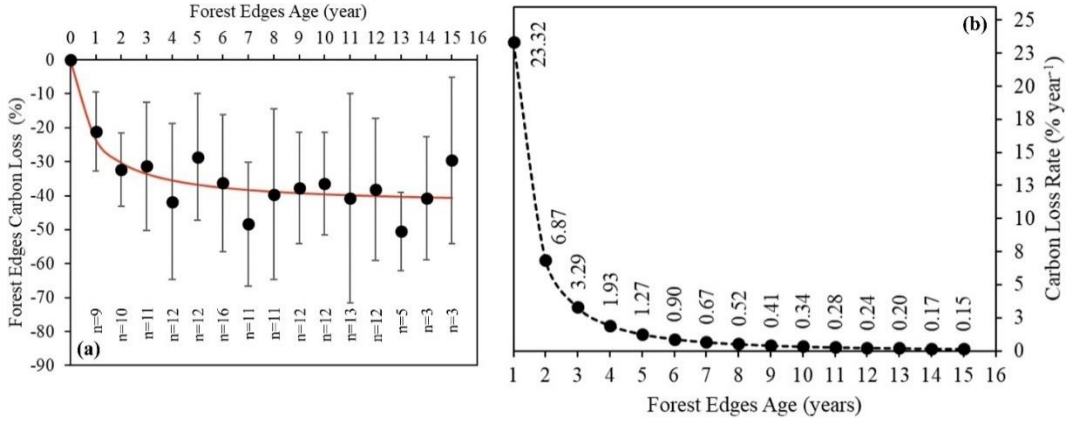


**Fig. S13. Above-Ground Carbon Stock Loss Model by Edge Effect. (a)** Fitting of the Michaelis-Menten kinetic curve on the measured values. **(b)** Carbon loss decay rate based on the model in Fig S13a.

**Table S5. Carbon loss factor (f) for the calculation of carbon loss from edge effect.**

| Forest Edges Ages (year) | Accumulated Carbon Loss (%) | Carbon Loss Rate (% year$^{-1}$) | Carbon Loss Factor (*f*) |
|---|---|---|---|
| 1 | 23.324 | 23.324 | 0.233 |
| 2 | 30.198 | 6.873 | 0.069 |
| 3 | 33.487 | 3.289 | 0.033 |
| 4 | 35.416 | 1.929 | 0.019 |
| 5 | 36.684 | 1.268 | 0.013 |
| 6 | 37.581 | 0.897 | 0.009 |
| 7 | 38.249 | 0.668 | 0.007 |
| 8 | 38.765 | 0.517 | 0.005 |
| 9 | 39.177 | 0.412 | 0.004 |
| 10 | 39.513 | 0.336 | 0.003 |
| 11 | 39.792 | 0.279 | 0.003 |
| 12 | 40.027 | 0.236 | 0.002 |
| 13 | 40.229 | 0.201 | 0.002 |
| 14 | 40.403 | 0.174 | 0.002 |
| 15 | 40.555 | 0.152 | 0.002 |

To extrapolate the percent changes in AGC stocks (carbon loss) from the forest edges, we first combined the annual age maps with a forest AGB density map a pixel-by-pixel approach (30-m spatial resolution), attributing to each edge pixel an initial (pre-edge formation) biomass value ($AGB_{Pixel}$). We carried out a similar procedure for the deforested pixels. We used the GFW (Global Forest Watch) forest biomass density map at 30-m spatial resolution, which was elaborated based on the method proposed by Baccini et al. (*1*) (https://data.globalforestwatch.org/datasets/aboveground-live-woody-biomass-density).

For estimating Amazonia-wide edge effect on carbon loss between 2001 and 2015, we applied Equation 3 for each pixel.

$$CL_{Pixel} = L_{Factor} \cdot AGB_{Pixel} \cdot 0.5 \cdot 0.09 \qquad (3)$$

where $CL_{Pixel}$ is the pixel carbon loss at the forest edges given in Mg per pixel, $L_{Factor}$ is the loss factor for each forest edge age, calculated based on equation 2a (Table S5), $AGB_{Pixel}$ is the pre-edge or pre-deforestation AGB value of the pixel, obtained by the previous integration step, 0.5 is the AGB to AGC conversion factor (*89*), and 0.09 is the conversion factor to transform carbon density in Mg ha$^{-1}$ to total carbon for the entire pixel area (0.09 ha).

For calculating the Amazonia-wide loss of C associated to the deforestation process, between 2001 and 2015, we applied Equation 4 for each pixel.

$$CL_{Pixel} = L_{Factor} \,.\, AGB_{Pixel} \cdot 0.5 \cdot 0.09 \qquad (4)$$

All terms in equation 4 are similar to those in equation 3, however, $L_{Factor}$ in this case is set to "1", indicating that all carbon stored in the pixel (100%) will be lost following the deforestation process.

Finally, to present in the maps the results of carbon losses across Amazonia associated to edge effect and deforestation, we aggregated all original pixels values at a 30-m spatial resolution into grid-cells with 10-km spatial resolution using the sum of the values.

**Statistical analysis**

Here we used nonparametric statistical approaches, for all analyses. For testing the temporal trends, we used the Mann-Kendall test and the Sen's Slope Estimator. To compare forest edges ages and carbon losses among Amazonian countries we used the Kruskal-Wallis test and the Wilcoxon test. All analyses were performed using the R statistical software (*88*) (version 3.4.4; https://www.r-project.org). For the Kruskal-Wallis and the Wilcoxon test, we used the "agricolae" package (*90*), whereas for the Mann-Kendall test and the Sen's Slope Estimator the "wq" package (*91*) was used. For all statistical analysis, we adopted the significance level of 95% ($p \leq 0.05$).

To analyse the temporal trend in deforestation rates, forest edge increment, and forest carbon loss, we used the Mann-Kendall test (*92*, *93*). Then we calculated the magnitude of the changes by the application of Sen's Slope method (*94*). The Mann-Kendall test is used to assess whether there is a monotonic upward or downward trend over a time period, whereas the Sen's Slope Estimator, a robust nonparametric method with little sensitivity to outliers, is used to estimate the magnitude of trends by the calculation of the median of the slopes of each pair of points in the data.

To verify the existence of significant differences in the forest edges ages among the Amazonian countries, we used the Kruskal-Wallis test (*95*). The Kruskal-Wallis test is equivalent to the Analysis of Variance (ANOVA), which compares three or more groups to test the hypothesis that they have the same distribution. To determine how the analysed variables, differ from each other, we performed a paired posthoc test. In the posthoc test, we used the Fisher's least significant difference criterion with Bonferroni adjustment methods correction (*96*).

Finally, to verify the existence of significant differences in carbon losses associated to edge effect and deforestation between the period before (between 2001 and 2004) and after (between 2005 and 2015) the PPCDAm (Action Plan for Prevention and Control of Deforestation in the Legal Amazon) (*36*) implementation, we used the Wilcoxon test for independent samples (*95*). The Wilcoxon test, which is equivalent to the Student's t-test, compares two independents groups to test the hypothesis that they have the same median. We use the Fisher's least significant difference criterion with Bonferroni adjustment methods correction (*96*).

**Sources of uncertainty**

Our estimations of carbon losses associated to edge effect and deforestation were performed from 2001 onwards due to the lack of forest-cover, forest-change, and biomass data for Amazonia before this period. Thus, our estimates do not account for historical carbon losses before 2001. In 2000 we estimate an area of edge-affected forests (including natural edges) of 416,793 $km^2$ (82% of the total edge area in 2015) within 120m of edge length, while accumulated deforestation in 2000 accounted for 591,414 $km^2$ (*43*) across Amazonia.

Regarding the accuracy of remote sensing products, the 2000 forest map produced from the 80% tree cover percentage threshold has an overall accuracy of 82% (*84*), while forest cover change data has an overall accuracy of 99.5% (*28*). The biomass map (*1*) used has uncertainties from allometric equations, the LiDAR-based model, and the random forest model; however, we used the latest and improved map with a low level of uncertainty (https://data.globalforestwatch.org/datasets/aboveground-live-woody-biomass-density).

The effective edge distance of 120 m used was based on the well-documented landscape scale experiment in Central Brazilian Amazon (Manaus state) published by Laurence et al. (*10*), although carbon loss may occur up to 300 m of edge (*10*), making our carbon loss estimates conservative. Moreover, the variation of the penetrability of the carbon collapse from the edge to the interior of the forest throughout Amazonia is still unknown, making unfeasible at this stage the implementation of a function representing this variation in our analyses. The fix edge distance of 120 m, hence, is the most appropriated threshold, as it is conservative, comparable with other studies (*21–23*) and with effects on forest biomass well documented in the literature. In our analysis, we assumed that the open and closed edges are equally impacted by edge effects, although these impacts may assume different magnitudes depending on the edge type, as suggested by Didham and Lawton (*61*).

Although our forest carbon loss estimates associated to edge effect consider a global model for the entire Amazon, our approach represents an advance in relation to previous studies (*21–26*), contributing to an improved understanding of the collateral impacts of deforestation on Amazonian carbon stocks. Finally, unlike previous studies (*21–26*), our estimates of carbon loss were based for the first time on samples derived from various regions of the Amazon, describing the gradual decay of carbon at forest edges over 15 years.

**REFERENCES AND NOTES**


1. A. Baccini, S. J. Goetz, W. S. Walker, N. T. Laporte, M. Sun, D. Sulla-Menashe, J. Hackler, P. S. A. Beck, R. Dubayah, M. A. Friedl, S. Samanta, R. A. Houghton, Estimated carbon dioxide emissions from tropical deforestation improved by carbon-density maps. *Nat. Clim. Chang.* **2**, 182–185 (2012).

2. S. S. Saatchi, N. L. Harris, S. Brown, M. Lefsky, E. T. A Mitchard, W. Salas, B. R. Zutta, W. Buermann, S. L. Lewis, S. Hagen, S. Petrova, L. White, M. Silman, A. Morel, Benchmark map of forest carbon stocks in tropical regions across three continents. *Proc. Natl. Acad. Sci. U.S.A.* **108**, 9899–9904 (2011).

3. Y. Y. Liu, A. I. J. M. van Dijk, R. A. M. de Jeu, J. G. Canadell, M. F. McCabe, J. P. Evans, G. Wang, Recent reversal in loss of global terrestrial biomass. *Nat. Clim. Chang.* **5**, 470–474 (2015).

4. R. J. Keenan, G. A. Reams, F. Achard, J. V. de Freitas, A. Grainger, E. Lindquist, Dynamics of global forest area: Results from the FAO Global Forest Resources Assessment 2015. *For. Ecol. Manag.* **352**, 9–20 (2015).

5. J. A. Foley, R. De Fries, G. P. Asner, C. Barford, G. Bonan, S. R. Carpenter, F. S. Chapin, M. T. Coe, G. C. Daily, H. K. Gibbs, J. H. Helkowski, T. Holloway, E. A. Howard, C. J. Kucharik, C. Monfreda, J. A. Patz, I. C. Prentice, N. Ramankutty, P. K. Snyder, Global consequences of land use. *Science* **309**, 570–574 (2005).

6. A. Baccini, W. Walker, L. Carvalho, M. Farina, D. Sulla-Menashe, R. A. Houghton, Tropical forests are a net carbon source based on aboveground measurements of gain and loss. *Science* **358**, 230–234 (2017).

7. L. B. Vedovato, M. G. Fonseca, E. Arai, L. O. Anderson, L. E. O. C. Aragão, The extent of 2014 forest fragmentation in the Brazilian Amazon. *Reg. Environ. Chang.* **16**, 2485–2490 (2016).

8. C. H. L. Silva Junior, L. E. O. C. Aragão, M. G. Fonseca, C. T. Almeida, L. B. Vedovato, L. O. Anderson, Deforestation-induced fragmentation increases forest fire occurrence in central Brazilian Amazonia. *Forests* **9**, 305 (2018).

9. L. V. Ferreira, W. F. Laurance, Effects of forest fragmentation on mortality and damage of selected trees in central Amazonia. *Conserv. Biol.* **11**, 797–801 (1997).

10. W. F. Laurance, S. G. Laurance, L. V. Ferreira, J. M. Rankin-de Merona, C. Gascon, T. E. Lovejoy, Biomass collapse in Amazonian forest fragments. *Science* **278**, 1117–1118 (1997).

11. H. E. M. Nascimento, W. F. Laurance, Biomass dynamics in Amazonian forest fragments. *Ecol. Appl.* **14**, 127–138 (2004).

12. E. N. Broadbent, G. P. Asner, M. Keller, D. E. Knapp, P. J. C. Oliveira, J. N. Silva, Forest fragmentation and edge effects from deforestation and selective logging in the Brazilian Amazon. *Biol. Conserv.* **141**, 1745–1757 (2008).

13. D. Armenteras, T. M. González, J. Retana, Forest fragmentation and edge influence on fire occurrence and intensity under different management types in Amazon forests. *Biol. Conserv.* **159**, 73–79 (2013).

14. R. Chaplin-Kramer, I. Ramler, R. Sharp, N. M. Haddad, J. S. Gerber, P. C. West, L. Mandle, P. Engstrom, A. Baccini, S. Sim, C. Mueller, H. King, Degradation in carbon stocks near tropical forest edges. *Nat. Commun.* **6**, 10158 (2015).

15. D. Armenteras, J. S. Barreto, K. Tabor, R. Molowny-Horas, J. Retana, Changing patterns of fire occurrence in proximity to forest edges, roads and rivers between NW Amazonian countries. *Biogeosciences* **14**, 2755–2765 (2017).

16. F. Taubert, R. Fischer, J. Groeneveld, S. Lehmann, M. S. Müller, E. Rödig, T. Wiegand, A. Huth, Global patterns of tropical forest fragmentation. *Nature* **554**, 519–522 (2018).

17. K. Riitters, J. Wickham, R. O'Neill, B. Jones, E. Smith, Global-scale patterns of forest fragmentation. *Conserv. Ecol.* **4**, 3 (2000).

18. M. C. Hansen, L. Wang, X.-P. Song, A. Tyukavina, S. Turubanova, P. V. Potapov, S. V. Stehman, The fate of tropical forest fragments. *Sci. Adv.* **6**, eaax8574 (2020).

19. N. M. Haddad, L. A. Brudvig, J. Clobert, K. F. Davies, A. Gonzalez, R. D. Holt, T. E. Lovejoy, J. O. Sexton, M. P. Austin, C. D. Collins, W. M. Cook, E. I. Damschen, R. M. Ewers, B. L. Foster, C. N. Jenkins, A. J. King, W. F. Laurance, D. J. Levey, C. R. Margules, B. A. Melbourne, A. O. Nicholls, J. L. Orrock, D.-X. Song, J. R. Townshend, Habitat fragmentation and its lasting impact on Earth's ecosystems. *Sci. Adv.* **1**, e1500052 (2015).

20. UNFCCC - United Nations Framework Convention on Climate Change, Forest reference emission levels (2019); https://redd.unfccc.int/fact-sheets/forest-reference-emission-levels.html.

21. I. Numata, M. A. Cochrane, D. A. Roberts, J. V. Soares, C. M. Souza Jr., M. H. Sales, Biomass collapse and carbon emissions from forest fragmentation in the Brazilian Amazon. *J. Geophys. Res.* **115**, G03027 (2010).

22. L. de Barros Viana Hissa, H. Müller, A. P. D. Aguiar, P. Hostert, T. Lakes, Historical carbon fluxes in the expanding deforestation frontier of Southern Brazilian Amazonia (1985–2012). *Reg. Environ. Chang.* **18**, 77–89 (2018).

23. I. Numata, M. A. Cochrane, C. M. Souza Jr., M. H. Sales, Carbon emissions from deforestation and forest fragmentation in the Brazilian Amazon. *Environ. Res. Lett.* **6**, 044003 (2011).

24. S. Pütz, J. Groeneveld, K. Henle, C. Knogge, A. C. Martensen, M. Metz, J. P. Metzger, M. C. Ribeiro, M. Dantas de Paula, A. Huth, Long-term carbon loss in fragmented Neotropical forests. *Nat. Commun.* **5**, 5037 (2014).

25. K. Brinck, R. Fischer, J. Groeneveld, S. Lehmann, M. Dantas De Paula, S. Pütz, J. O. Sexton, D. Song, A. Huth, High resolution analysis of tropical forest fragmentation and its impact on the global carbon cycle. *Nat. Commun.* **8**, 14855 (2017).

26. S. L. Maxwell, T. Evans, J. E. M. Watson, A. Morel, H. Grantham, A. Duncan, N. Harris, P. Potapov, R. K. Runting, O. Venter, S. Wang, Y. Malhi, Degradation and forgone removals increase the carbon impact of intact forest loss by 626%. *Sci. Adv.* **5**, eaax2546 (2019).

27. D. R. A. Almeida, S. C. Stark, J. Schietti, J. L. C. Camargo, N. T. Amazonas, E. B. Gorgens, D. M. Rosa, M. N. Smith, R. Valbuena, S. Saleska, A. Andrade, R. Mesquita, S. G. Laurance, W. F. Laurance, T. E. Lovejoy, E. N. Broadbent, Y. E. Shimabukuro, G. G. Parker, M. Lefsky, C. A. Silva, P. H. S. Brancalion, Persistent effects of fragmentation on tropical rainforest canopy structure after 20 yr of isolation. *Ecol. Appl.* **29**, e01952 (2019).

28. M. C. Hansen, P. V. Potapov, R. Moore, M. Hancher, S. A. Turubanova, A. Tyukavina, D. Thau, S. V. Stehman, S. J. Goetz, T. R. Loveland, A. Kommareddy, A. Egorov, L. Chini, C. O. Justice, J. R.

G. Townshend, High-resolution global maps of 21st-century forest cover change. *Science* **342**, 850–853 (2013).

29. M. Longo, M. Keller, M. N. dos-Santos, V. Leitold, E. R. Pinagé, A. Baccini, S. Saatchi, E. M. Nogueira, M. Batistella, D. C. Morton, Aboveground biomass variability across intact and degraded forests in the Brazilian Amazon. *Glob. Biogeochem. Cycles* **30**, 1639–1660 (2016).

30. M. A. Lefsky, W. B. Cohen, G. G. Parker, D. J. Harding, Lidar remote sensing for ecosystem studies. *Bioscience* **52**, 19–30 (2002).

31. E. M. Ordway, G. P. Asner, Carbon declines along tropical forest edges correspond to heterogeneous effects on canopy structure and function. *Proc. Natl. Acad. Sci. U.S.A.* **117**, 7863–7870 (2020).

32. M. Melito, J. P. Metzger, A. A. de Oliveira, Landscape-level effects on aboveground biomass of tropical forests: A conceptual framework. *Glob. Chang. Biol.* **24**, 597–607 (2018).

33. I. Numata, S. S. Silva, M. A. Cochrane, M. V. N. d'Oliveira, Fire and edge effects in a fragmented tropical forest landscape in the southwestern Amazon. *For. Ecol. Manag.* **401**, 135–146 (2017).

34. M. D. Velasco Gomez, R. Beuchle, Y. Shimabukuro, R. Grecchi, D. Simonetti, H. D. Eva, F. Achard, A long-term perspective on deforestation rates in the Brazilian Amazon. *ISPRS* **XL-7/W3**, 539–544 (2015).

35. Instituto Nacional de Pesquisas Espaciais (INPE), PRODES - Monitoramento da floresta amazônica brasileira por satélite (2020); http://www.obt.inpe.br/OBT/assuntos/programas/amazonia/prodes.

36. Ministério do Meio Ambiente (MMA), *Plano de Ação para prevenção e controle do desmatamento na Amazônia Legal (PPCDAm): 3$^{a}$ fase (2012-2015) pelo uso sustentável e conservação da Floresta* (MMA, Brasíla, 2013); http://combateaodesmatamento.mma.gov.br/images/conteudo/PPCDAM_3aFase.pdf.

37. N. G. R. de Mello, P. Artaxo, Evolução do Plano de Ação para Prevenção e Controle do Desmatamento na Amazônia Legal. *Rev. do Inst. Estud. Bras.*, 108–129 (2017).

38. P. H. S. Brancalion, L. C. Garcia, R. Loyola, R. R. Rodrigues, V. D. Pillar, T. M. Lewinsohn, A critical analysis of the Native Vegetation Protection Law of Brazil (2012): Updates and ongoing initiatives. *Nat. Conserv.* **14**, 1–15 (2016).

39. J. Barlow, E. Berenguer, R. Carmenta, F. França, Clarifying Amazonia's burning crisis. *Glob. Chang. Biol.* **26**, 319–321 (2020).

40. Associação Nacional dos Servidores de Meio Ambiente (ASCEMA), Cronologia de um desastre anunciado: Ações do governo Bolsonaro para desmontar as políticas de meio ambiente no Brasil (2020); http://www.ascemanacional.org.br/wp-content/uploads/2020/09/Dossie_Meio-Ambiente_Governo-Bolsonaro_revisado_02-set-2020-1.pdf.

41. D. Nepstad, D. McGrath, C. Stickler, A. Alencar, A. Azevedo, B. Swette, T. Bezerra, M. DiGiano, J. Shimada, R. Seroa da Motta, E. Armijo, L. Castello, P. Brando, M. C. Hansen, M. McGrath-Horn, O. Carvalho, L. Hess, Slowing Amazon deforestation through public policy and interventions in beef and soy supply chains. *Science* **344**, 1118–1123 (2014).

42. V. López Acevedo, Ecuador: Rainforest under siege, in *The 21st Century Fight for the Amazon*, M. Ungar, Ed. (Springer International Publishing, Cham, 2018), pp. 93–113.

43. RAISG - Amazonian Network of Georeferenced Socio-Environmental Information, Deforestation in the Amazonia (1970–2013) (2015); https://www.amazoniasocioambiental.org/en/download/deforestation-in-the-amazonia-1970-2013-atlas/.

44. C. Dezécache, E. Faure, V. Gond, J.-M. Salles, G. Vieilledent, B. Hérault, Gold-rush in a forested El Dorado: Deforestation leakages and the need for regional cooperation. *Environ. Res. Lett.* **12**, 034013 (2017).

45. K. Delvoye, M. Parahoe, H. Libretto, Suriname: An exposed interior, in *The 21st Century Fight for the Amazon*, M. Ungar, Ed. (Springer International Publishing, Cham, 2018), pp. 149–170.

46. G. P. Asner, R. Tupayachi, Accelerated losses of protected forests from gold mining in the Peruvian Amazon. *Environ. Res. Lett.* **12**, 094004 (2016).

47. M. K. Steininger, C. J. Tucker, J. R. G. Townshend, T. J. Killeen, A. Desch, V. Bell, P. Ersts, Tropical deforestation in the Bolivian Amazon. *Environ. Conserv.* **28**, 127–134 (2001).

48. D. Armenteras, G. Rudas, N. Rodriguez, S. Sua, M. Romero, Patterns and causes of deforestation in the Colombian Amazon. *Ecol. Indic.* **6**, 353–368 (2006).

49. W. F. Laurance, J. L. C. Camargo, P. M. Fearnside, T. E. Lovejoy, G. B. Williamson, R. C. G. Mesquita, C. F. J. Meyer, P. E. D. Bobrowiec, S. G. W. Laurance, An Amazonian rainforest and its fragments as a laboratory of global change. *Biol. Rev.* **93**, 223–247 (2018).

50. I. Numata, M. A. Cochrane, D. A. Roberts, J. V. Soares, Determining dynamics of spatial and temporal structures of forest edges in South Western Amazonia. *For. Ecol. Manag.* **258**, 2547–2555 (2009).

51. W. F. Laurance, S. G. Laurance, P. Delamonica, Tropical forest fragmentation and greenhouse gas emissions. *For. Ecol. Manag.* **110**, 173–180 (1998).

52. M. Kalamandeen, E. Gloor, E. Mitchard, D. Quincey, G. Ziv, D. Spracklen, B. Spracklen, M. Adami, L. E. O. C. Aragão, D. Galbraith, Pervasive rise of small-scale deforestation in Amazonia. *Sci. Rep.* **8**, 1600 (2018).

53. W. F. Laurance, P. Delamônica, S. G. Laurance, H. L. Vasconcelos, T. E. Lovejoy, Rainforest fragmentation kills big trees. *Nature* **404**, 836 (2000).

54. P. M. Brando, J. K. Balch, D. C. Nepstad, D. C. Morton, F. E. Putz, M. T. Coe, D. Silverio, M. N. Macedo, E. A. Davidson, C. C. Nóbrega, A. Alencar, B. S. Soares-Filho, Abrupt increases in Amazonian tree mortality due to drought-fire interactions. *Proc. Natl. Acad. Sci. U.S.A.* **111**, 6347–6352 (2014).

55. V. Kapos, Effects of isolation on the water status of forest patches in the Brazilian Amazon. *J. Trop. Ecol.* **5**, 173–185 (1989).

56. J. L. C. Camargo, V. Kapos, Complex edge effects on soil moisture and microclimate in central Amazonian forest. *J. Trop. Ecol.* **11**, 205–221 (1995).

57. R. Trancoso, thesis, National Institute for Amazonian Research - INPA, Manaus (2008).

58. N. Sizer, E. V. J. Tanner, Responses of woody plant seedlings to edge formation in a lowland tropical rainforest, Amazonia. *Biol. Conserv.* **91**, 135–142 (1999).

59. T. E. Lovejoy, R. O. Bierregaard, A. B. Rylands, J. R. Malcom, C. E. Quintela, L. H. Harper, K. S. Brown Jr., A. H. Powell, G. V. N. Powell, H. O. R. Schubart, M. B. Hays, in *Conservation Biology: The Science of Scarcity and Diversity*, M. E. Soulé, Ed. (Sinauer Press, Massachusetts, 1986), pp. 257–285.

60. W. F. Laurance, L. V. Ferreira, J. M. Rankin-de Merona, S. G. Laurance, Rain forest fragmentation and the dynamics of Amazonian tree communities. *Ecology* **79**, 2032–2040 (1998).

61. R. K. Didham, J. H. Lawton, Edge structure determines the magnitude of changes in microclimate and vegetation structure in tropical forest fragments. *Biotropica* **31**, 17–30 (1999).

62. S. A. D'Angelo, A. C. S. Andrade, S. G. Laurance, W. F. Laurance, R. C. G. Mesquita, Inferred causes of tree mortality in fragmented and intact Amazonian forests. *J. Trop. Ecol.* **20**, 243–246 (2004).

63. W. F. Laurance, H. E. M. Nascimento, S. G. Laurance, A. C. Andrade, P. M. Fearnside, J. E. L. Ribeiro, R. L. Capretz, Rain forest fragmentation and the proliferation of successional trees. *Ecology* **87**, 469–482 (2006).

64. C. V. J. Silva, L. E. O. C. Aragão, J. Barlow, F. Espirito-Santo, P. J. Young, L. O. Anderson, E. Berenguer, I. Brasil, I. Foster Brown, B. Castro, R. Farias, J. Ferreira, F. França, P. M. L. A. Graça, L. Kirsten, A. P. Lopes, C. Salimon, M. A. Scaranello, M. Seixas, F. C. Souza, H. A. M. Xaud, Drought-induced Amazonian wildfires instigate a decadal-scale disruption of forest carbon dynamics. *Philos. Trans. R. Soc. B* **373**, 20180043 (2018).

65. C. H. L. Silva Junior, V. H. A. Heinrich, A. T. G. Freire, I. S. Broggio, T. M. Rosan, J. Doblas, L. O. Anderson, G. X. Rousseau, Y. E. Shimabukuro, C. A. Silva, J. I. House, L. E. O. C. Aragão, Benchmark maps of 33 years of secondary forest age for Brazil. *Sci. Data* **7**, 269 (2020).

66. R. C. G. Mesquita, P. Delamônica, W. F. Laurance, Effect of surrounding vegetation on edge-related tree mortality in Amazonian forest fragments. *Biol. Conserv.* **91**, 129–134 (1999).

67. M. A. Cochrane, Synergistic interactions between habitat fragmentation and fire in evergreen tropical forests. *Conserv. Biol.* **15**, 1515–1521 (2001).

68. M. A. Cochrane, W. F. Laurance, Fire as a large-scale edge effect in Amazonian forests. *J. Trop. Ecol.* **18**, 311–325 (2002).

69. M. A. Cochrane, W. F. Laurance, Synergisms among fire, land use, and climate change in the Amazon. *AMBIO* **37**, 522–527 (2008).

70. A. Cano-Crespo, P. J. C. Oliveira, A. Boit, M. Cardoso, K. Thonicke, Forest edge burning in the Brazilian Amazon promoted by escaping fires from managed pastures. *J. Geophys. Res. Biogeosci.* **120**, 2095–2107 (2015).

71. L. E. O. C. Aragão, Y. Malhi, N. Barbier, A. Lima, Y. Shimabukuro, L. Anderson, S. Saatchi, Interactions between rainfall, deforestation and fires during recent years in the Brazilian Amazonia. *Philos. Trans. R. Soc. Lond. Ser. B Biol. Sci.* **363**, 1779–1785 (2008).

72. D. V. Silvério, P. M. Brando, M. M. C. Bustamante, F. E. Putz, D. M. Marra, S. R. Levick, S. E. Trumbore, Fire, fragmentation, and windstorms: A recipe for tropical forest degradation. *J. Ecol.* **107**, 656–667 (2019).

73. J. A. Marengo, C. M. Souza Jr., K. Thonicke, C. Burton, K. Halladay, R. A. Betts, L. M. Alves, W. R. Soares, Changes in climate and land use over the Amazon region: Current and future variability and trends. *Front. Earth Sci.* **6**, 228 (2018).

74. J. A. Marengo, J. C. Espinoza, Extreme seasonal droughts and floods in Amazonia: Causes, trends and impacts. *Int. J. Climatol.* **36**, 1033–1050 (2016).

75. R. J. W. Brienen, O. L. Phillips, T. R. Feldpausch, E. Gloor, T. R. Baker, J. Lloyd, G. Lopez-Gonzalez, A. Monteagudo-Mendoza, Y. Malhi, S. L. Lewis, R. Vásquez Martinez, M. Alexiades, E. Álvarez Dávila, P. Alvarez-Loayza, A. Andrade, L. E. O. C. Aragão, A. Araujo-Murakami, E. J. M. M. Arets, L. Arroyo, G. A. Aymard C, O. S. Bánki, C. Baraloto, J. Barroso, D. Bonal, R. G. A. Boot, J. L. C. Camargo, C. V. Castilho, V. Chama, K. J. Chao, J. Chave, J. A. Comiskey, F. Cornejo Valverde, L. da Costa, E. A. de Oliveira, A. Di Fiore, T. L. Erwin, S. Fauset, M. Forsthofer, D. R. Galbraith, E. S. Grahame, N. Groot, B. Hérault, N. Higuchi, E. N. Honorio Coronado, H. Keeling, T.

J. Killeen, W. F. Laurance, S. Laurance, J. Licona, W. E. Magnussen, B. S. Marimon, B. H. Marimon-Junior, C. Mendoza, D. A. Neill, E. M. Nogueira, P. Núñez, N. C. Pallqui Camacho, A. Parada, G. Pardo-Molina, J. Peacock, M. Peña-Claros, G. C. Pickavance, N. C. A. Pitman, L. Poorter, A. Prieto, C. A. Quesada, F. Ramírez, H. Ramírez-Angulo, Z. Restrepo, A. Roopsind, A. Rudas, R. P. Salomão, M. Schwarz, N. Silva, J. E. Silva-Espejo, M. Silveira, J. Stropp, J. Talbot, H. ter Steege, J. Teran-Aguilar, J. Terborgh, R. Thomas-Caesar, M. Toledo, M. Torello-Raventos, R. K. Umetsu, G. M. F. van der Heijden, P. van der Hout, I. C. Guimarães Vieira, S. A. Vieira, E. Vilanova, V. A. Vos, R. J. Zagt, Long-term decline of the Amazon carbon sink. *Nature* **519**, 344–348 (2015).

76. L. E. O. C. Aragão, Y. Malhi, R. M. Roman-Cuesta, S. Saatchi, L. O. Anderson, Y. E. Shimabukuro, Spatial patterns and fire response of recent Amazonian droughts. *Geophys. Res. Lett.* **34**, L07701 (2007).

77. L. E. O. C. Aragão, L. O. Anderson, M. G. Fonseca, T. M. Rosan, L. B. Vedovato, F. H. Wagner, C. V. J. Silva, C. H. L. Silva Junior, E. Arai, A. P. Aguiar, J. Barlow, E. Berenguer, M. N. Deeter, L. G. Domingues, L. Gatti, M. Gloor, Y. Malhi, J. A. Marengo, J. B. Miller, O. L. Phillips, S. Saatchi, 21st century drought-related fires counteract the decline of Amazon deforestation carbon emissions. *Nat. Commun.* **9**, 536 (2018).

78. C. H. L. Silva Junior, L. O. Anderson, A. L. Silva, C. T. Almeida, R. Dalagnol, M. A. J. S. Pletsch, T. V. Penha, R. A. Paloschi, L. E. O. C. Aragão, Fire responses to the 2010 and 2015/2016 Amazonian droughts. *Front. Earth Sci.* **7**, 97 (2019).

79. UNFCCC - Framework Convention on Climate Change, The Paris Agreement (2015); https://unfccc.int/process-and-meetings/the-paris-agreement/the-paris-agreement.

80. IPCC - Intergovernmental Panel on Climate Change, Special Report on Global Warming of 1.5°C: Summary for Policymakers (2018); https://www.ipcc.ch/sr15/chapter/spm/.

81. V. Masson-Delmotte, P. Zhai, H.-O. Pörtner, D. Roberts, J. Skea, P. R. Shukla, A. Pirani, W. Moufouma-Okia, C. Péan, R. Pidcock, S. Connors, J. B. R. Matthews, Y. Chen, X. Zhou, M. I. Gomis, E. Lonnoy, T. Maycock, M. Tignor, T. Waterfield, *Global Warming of 1.5 °C: Summary for Policymakers* (World Meteorological Organization, 2018).

82. H. D. Eva, O. Huber, F. Achard, H. Balslev, S. Beck, H. Behling, A. S. Belward, R. Beuchle, A. Cleef, M. Colchester, J. Duivenvoorden, M. Hoogmoed, W. Junk, P. Kabat, B. Kruijt, Y. Malhi, J. M. Müller, J. M. Pereira, C. Peres, G. T. Prance, J. Roberts, J. Salo, *A Proposal for Defining the Geographical Boundaries of Amazonia* (Publications Office, Luxembourg, 2005).

83. J.-F. Pekel, A. Cottam, N. Gorelick, A. S. Belward, High-resolution mapping of global surface water and its long-term changes. *Nature* **540**, 418–422 (2016).

84. K. A. C. Gasparini, C. H. L. Silva Junior, Y. E. Shimabukuro, E. Arai, L. E. O. C. Aragão, C. A. Silva, P. L. Marshall, Determining a threshold to delimit the Amazonian Forests from the Tree Canopy Cover 2000 GFC Data. *Sensors* **19**, 5020 (2019).

85. P.-E. Danielsson, Euclidean distance mapping. *Comput. Graph. Image Process.* **14**, 227–248 (1980).

86. V. Leitold, M. Keller, D. C. Morton, B. D. Cook, Y. E. Shimabukuro, Airborne lidar-based estimates of tropical forest structure in complex terrain: Opportunities and trade-offs for REDD+. *Carbon Balance Manag.* **10**, 3 (2015).

87. D. Kushary, Bootstrap methods and their application. *Technometrics* **42**, 216–217 (2000).

88. R Core Team, R: A language and environment for statistical computing. R Foundation for Statistical Computing, Vienna, Austria (2020); https://www.r-project.org.

89. J. Chave, C. Andalo, S. Brown, M. A. Cairns, J. Q. Chambers, D. Eamus, H. Fölster, F. Fromard, N. Higuchi, T. Kira, J.-P. Lescure, B. W. Nelson, H. Ogawa, H. Puig, B. Riéra, T. Yamakura, Tree allometry and improved estimation of carbon stocks and balance in tropical forests. *Oecologia* **145**, 87–99 (2005).

90. F. de Mendiburu, Package 'agricolae', in *Statistical Procedures for Agricultural Research* (2017), pp. 157.

91. A. D. Jassby, J. E. Cloern, Package 'wq' (2016), pp. 42.

92. M. G. Kendall, *Rank Correlation Methods* (Charles Griffin, London, 1975).

93. H. B. Mann, Nonparametric tests against trend. *Econometrica* **13**, 245–259 (1945).

94. P. K. Sen, Estimates of the regression coefficient based on Kendall's tau. *J. Am. Stat. Assoc.* **63**, 1379–1389 (1968).

95. T. P. Hettmansperger, J. W. McKean, *Robust Nonparametric Statistical Methods* (CRC Press, ed. 2, 2010).

96. W. J. Conover, *Practical Nonparametric Statistics* (John Wiley & Sons, ed. 3, 1999).